Accepted Manuscript

Discovery of dehydroabietic acid sulfonamide based derivatives as selective matrix metalloproteinases inactivators that inhibit cell migration and proliferation

Ri-Zhen Huang, Gui-Bin Liang, Xiao-Chao Huang, Bin Zhang, Mei-Mei Zhou, Zhi-Xin Liao, Heng-Shan Wang

PII: S0223-5234(17)30542-1

DOI: 10.1016/j.ejmech.2017.07.020

Reference: EJMECH 9583

To appear in: *European Journal of Medicinal Chemistry*

Received Date: 24 May 2017

Revised Date: 11 July 2017

Accepted Date: 12 July 2017

Please cite this article as: R.-Z. Huang, G.-B. Liang, X.-C. Huang, B. Zhang, M.-M. Zhou, Z.-X. Liao, H.-S. Wang, Discovery of dehydroabietic acid sulfonamide based derivatives as selective matrix metalloproteinases inactivators that inhibit cell migration and proliferation, *European Journal of Medicinal Chemistry* (2017), doi: 10.1016/j.ejmech.2017.07.020.

Graphical abstract

Discovery of dehydroabietic acid sulfonamide based derivatives as selective matrix metalloproteinases inactivators that inhibit cell migration and proliferation

Ri-Zhen Huang, Gui-Bin Liang, Xiao-Chao Huang, Bin Zhang, Zhi-Xin Liao, and Heng-Shan Wang

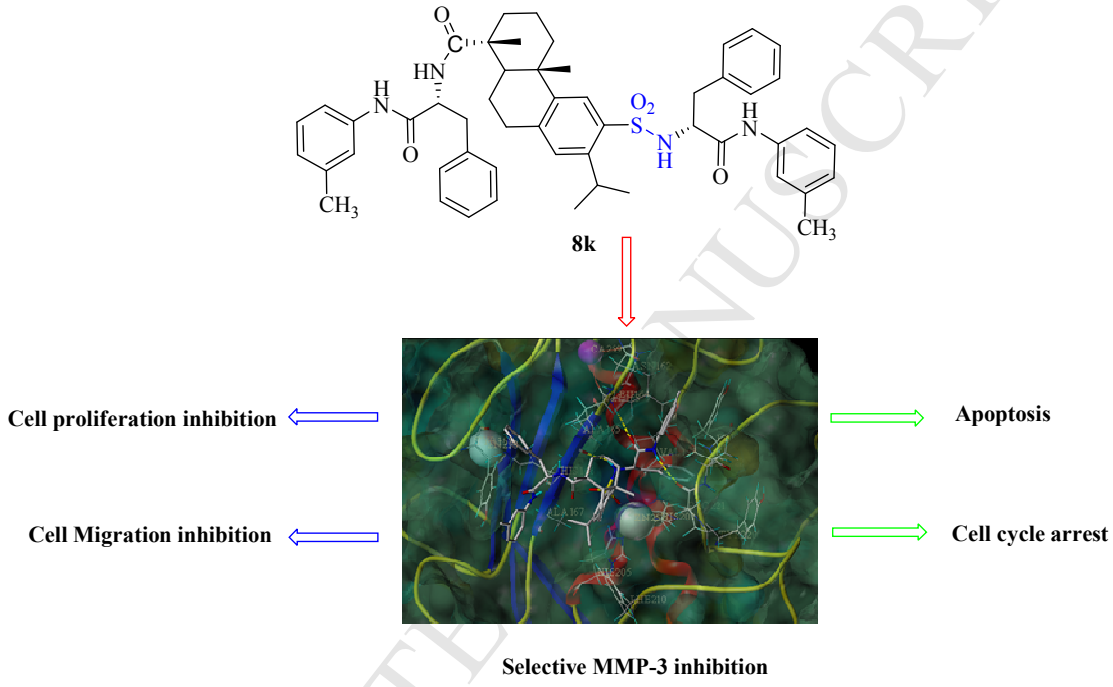

Discovery of dehydroabietic acid sulfonamide based derivatives as selective matrix metalloproteinases inactivators that inhibit cell migration and proliferation

Ri-Zhen Huang[a, 1], Gui-Bin Liang[b, 1], Xiao-Chao Huang[a], Bin Zhang[b], Mei-Mei Zhou[b], Zhi-Xin Liao[a*], and Heng-Shan Wang[b*]

[a] *Pharmaceutical Research Center and School of Chemistry and Chemical Engineering, Southeast University, Nanjing 211189, China*

[b] *State Key Laboratory for the Chemistry and Molecular Engineering of Medicinal Resources (Ministry of Education of China), School of Chemistry and Pharmaceutical Sciences of Guangxi Normal University, Guilin 541004, PR China*

* Corresponding author.

*Corresponding author. E-mail addresses: zxliao@seu.edu.cn (Z.-X. Liao), whengshan@163.com (H. -S. Wang).

[1] Co-first author: These authors contributed equally to this work.

Abstract

A series of dehydroabietic acid (DHAA) dipeptide derivatives containing the sulfonamide moiety were designed, synthesized and evaluated for inhibition of MMPs as well as the effects of *in vitro* cell migration. These compounds exhibited relatively good inhibition activity against MMPs with IC_{50} values in low micromolar range. A docking study of the most active compound **8k** revealed key interactions between **8k** and MMP-3 in which the sulfonamide moiety and the dipeptide group were important for improving activity. It is noteworthy that further antitumor activity screening revealed that some compounds exhibited better inhibitory activity than the commercial anticancer drug 5-FU. In particular, compound **8k** appeared to be the most potent compound against the HepG2 cell line, at least partly, by inhibition of the activity of MMP-3 and apoptosis induction. The treatment of HepG2 cells with compound **8k** resulted in inhibition of *in vitro* cell migration through wound healing assay and G1 phase of cell cycle arrested. In addition, **8k**-induced apoptosis was significantly facilitated in HepG2 cells. Thus, we conclude that DHAA dipeptide derivatives containing the sulfonamide moiety may be the potential MMPs inhibitors with the ability to suppress cells migration.

keywords: Dehydroabietic acid; Dipeptide; Sulfonamide; Matrix metalloproteinases; Migration

1. Introduction

Cancer metastasis, the essential hallmarks of cancer, is initiated by migration and invasion of cancer cells [1]. Metastasis has been a major impediment to effective cancer treatment with conventional chemotherapeutic drugs and has been the leading cause of cancer-associated death in several cancers including liver, breast and lung cancers. Notably, several proteins play important role to initiate or repress cancer metastasis such as matrix metalloproteinases (MMPs) [2]. Therefore, targeting pivotal inhibition of metastasis-associated proteins or signaling pathways are the critical point for efficient cancer treatment.

The MMPs, which play a crucial role in many normal physiological functions, are a group of structurally related zinc-dependent endopeptidases involved in the degradation of extracellular matrix (ECM) components and a diverse array of non-ECM proteins [3]. Recent studies revealed that MMPs frequently up-regulated in cancer cells, facilitated migration and have a significant effect on the ability of cancer cells to grow in a secondary site [4-6]. It is also well-known that MMPs participate in several steps of cancer progression, including cancer cell growth, apoptosis, migration, invasion, and angiogenesis, thereby playing a key role in the development of human breast, colon, thyroid, lung, and prostate cancers [7, 8]. In particular, stromelysin-1 (MMP-3) has been the subject of intense research due to its presence in the vicinity of melanomas and metastatic tumors associated with breast cancer; it also functions as an active precursor to the action of other endopeptidases [9-11]. Therefore, MMPs could serve as promising targets for the development of new therapeutics to suppress cancer metastasis and down-regulation the expressions of MMPs may have benefits in enhancing the efficacy of anticancer drugs. Some MMPs inhibitors have been employed as sensitizers in the established cancer therapy over recent years. Despite evident and convincing data, indicating that MMP inhibitors have a high potential in clinical trial for cancer [12], their use in the clinic has been stalled due to their limited proof of efficacy and their adverse side effects, which might be related to insufficient target validation [13-15]. In this reason, gaining selectivity between the metalloproteases without decreasing inhibitory potency is a primary goal in the development of MMP inhibitors, which would help to improve their efficacy and avoid undesirable side effects.

Dehydroabietic acid (DHAA) is a naturally occurring diterpenic resin acid and has been found to exhibit a broad spectrum of biological activities, especially anticancer activities [16-19].

Moreover, previous research has shown that DHAA derivatives could act at various stages of tumor development to inhibit tumor initiation and promotion, as well as to induce tumor cell differentiation and apoptosis [20-22]. These findings suggest that DHAA may be a promising starting tool for the discovery of new anticancer agents. On the other hand, sulfonamides are currently an important group of organic compounds and have been reported for potent antitumor activity against numerous types of cancers [23, 24]. Derivatives containing sulfonamides moiety have been widely used as MMPs or carbonic anhydrase inhibitors, some of which are already in clinical trial [25-28] (Fig.1). Also, from the literature survey it was found that aryl sulfonamides might act as antitumor agents through several mechanisms [29]. Furthermore, peptides, which are among the most versatile bioactive molecules, have been reported to act as the inhibitors of some proteins and to exert their action by binding to membrane receptors [30-32]. In the present work, we designed and synthesized a series of DHAA dipeptide sulfonamides derivatives as selective MMPs inhibitors which suppress the migration of liver cancer cells. A docking analysis using the crystal structure of the MMP-3 was performed to clarify the binding mode of the designed inhibitors. Moreover, growth inhibitory effects of these compounds were evaluated against four human tumor cell lines. The migration inhibition, apoptosis inducing effects and cell cycle arrest in HepG2 cells by the representative target compound **8k** was also investigated.

2. Results and Discussion

2.1 Chemistry

The general procedures for the synthesis of DHAA dipeptide sulfonamides derivatives are shown in Scheme 1. As shown in Scheme 1, compound **3** was synthesized by the treatment of phenylalanine **1** with phthalic anhydride (**2**) in the presence of acetic acid according to the literature [33]. Compound **4** was then obtained by the condensation of compound **3** and oxalyl chloride, followed by treatment with series of aromatic primary amines. Compounds **5** were synthesized by the treatment of compounds **4** with hydrazine hydrate in the presence of ethanol at room temperature. Compound **6** was synthesized by the treatment of dehydroabietic acid with vitriol at room temperature [34]. Compound **6** was treated with oxalyl chloride to offer compound **7**. Compounds **8** were finally acquired by the condensation of compound **7** and compounds **5** (1:2) for 18 h in the presence of triethylamine at room temperature. Compounds **9** were finally acquired by the condensation of compound **7** and compounds **5** (1:1) for 6 h in the presence of

triethylamine at room temperature. The structures of target compounds **8** and **9** were then confirmed by ^{1}H NMR, ^{13}C NMR and high resolution mass spectrometry (HRMS).

2.2 Biological evaluation

2.2.1 In Vitro MMPs Assays

The synthesized DHAA derivatives containing sulfonamide dipeptide moiety were assayed in vitro against human recombinant MMP-3, MMP-8 and MMP-9 using synthetic fluorogenic substrates according to a previously reported procedure [35]. The broad spectrum inhibitor CGS-27023A was taken as positive control. The IC_{50} values obtained in the performed *in vitro* inhibition assays of DHAA derivatives are summarized in Table 1.

As shown in Table 1, the newly synthesized DHAA derivatives are potent MMPs inhibitors, with IC_{50} values mostly in micromolar or submicromolar levels. As can be seen from Table 1, the sulfonic acid group in compounds **9** formed a sulfonamide to give compounds **8**, substantially increased MMPs inhibitory activities, which may be due to sulfonamides derivatives were more active than sulfonic acid derivatives. Notably, when comparing the inhibitory activities of the different DHAA derivatives toward the investigated MMPs, most of the compounds were found to preferentially inhibit MMP-3. It was established that the structure of the lipophilic group as well as the configuration of the dipeptide scaffold significantly affected MMP inhibitory activity and selectivity. Among them, the most potent MMP-3 inhibitor, compound **8k** bearing a lipophilic methyl, effectively inhibited MMP-3 in the submicromolar range (IC_{50} = 0.4 μM), with selectivities over the other tested MMPs ranging from 6.6 to 8.8. The effects of the configuration of amino acid showed that the $_{L-}$ amino acid group generally enhanced MMP-3 inhibition, compared with a $_{D-}$ amino acid. Thus, compound **8n** showed weak inhibition against MMP-3, MMP-8 and -9 in the micromolar range. In contrast, its diastereomer **8o**, possessing an $_{L-}$ amino acid scaffold, was strikingly 2.5−33.5-fold more active toward all three tested MMPs with IC_{50} 1.0, 17.7, 20.9 μM against MMP-3, MMP-8, MMP-9, respectively. On the other hand, analysis of the effects of the terminal substituents at the R_1 position of dipeptide moiety showed that a methyl group generally enhanced MMP-3 inhibition, compared with a bromine or fluorine group substitution. When the bromine of compound **8e** was replaced with a methyl group at the 3-position on the phenyl ring (compound **8k**), the inhibitory potency was increased by 90-fold against MMP3 when compared to **8e**. Replacing the 4-position on the phenyl ring with a methyl

group at R_1 to yield compound **8n** and **8o**, respectively, resulted in a marked increase in potency, thus demonstrating that the lipophilic properties of the substituents may play a critical role in the inhibitory activities against MMP-3. However, the introduction of a fluorine group hindered the inhibitory activity. Moreover, analogs with a chlorine and fluorine fragments at R_1 were much less active or completely inactive. A variation at R_1 could cause a substantial difference in inhibitory potency, presumably due to different affinity to the binding pocket. Moreover, by the comparison of IC_{50} values of different position substituent, it also demonstrated that *meta*- or *para*-substituent at R_1 will enhance inhibition activities.

2.2.2. Molecular docking

To understand the interactions between the most active compound **8k** and the target of interest (MMP-3), we performed molecular docking calculations on the active site of MMP-3 using SYBYL-X 2.0 software and the results are summarized in Fig. 2 and Table 2. The interacting mode of compound **8k** (docking score 11.09), with the best docking score and interaction in the binding site of the MMP-3 receptor, is described and shown in Fig. 2a. Some key residues, such as LEU164, ALA165, HIS205, TYR223 and PRO221, as well as hydrogen bonds between the selected compound and the residues are also labeled. As shown in Fig. 2a, compound **8k** was stabilized predominantly by hydrogen-bond formation with the hydrophilic or hydrophobic groups of TYR155, LEU164, VAL198, TYR220 and PRO221. The sulfonamide group, which is the primary important moiety, formed a hydrogen-bond with the HIS166 carbonyl oxygen of the active site. More important, the sulfonamide moiety coordinates the catalytic zinc atom in a monodentate fashion (Fig. 2a). Furthermore, the carbonyl oxygen of the dipeptide group in the sulfonamide chain as an acceptor established one hydrogen bond with LEU164. In addition, the polar hydrogen of the amide moiety formed a hydrogen bond with the backbone carbonyl of PRO221, which confirmed that this moiety is also crucial for binding. The benzyl group of compound **8k** plunge deeply into S1'pocket, the enzyme's specificity pocket of MMP-3 in the same fashion as the binding mode of the ligand. In here, the benzyl ring is engaged in multiple hydrophobic interactions with VAL198, HIS201, TYR220, PRO221, LEU222 and TYR223 side chains. The methyl-aniline group is found sandwiched between ASN162 and LEU222, whereas the DHAA moiety is flanked by lipophilic residues such as HIS205 and PHE210. Clearly, all these interactions endow **8k** with a low micromolar inhibitory activity toward MMP-3. The binding

mode of 1SLN-ligand in the MMP-3 binding pocket is shown in Fig. 2b. Hydrogen bonds with LEU164, GLU202, PRO221 and TYR223 of MMP-3 were observed in the docked structure.

2.2.3 Cytotoxicity Measurement

The *in vitro* antiproliferative activity of the DHAA derivatives was evaluated by MTT assay against NCI-H46, HepG2, SKOV-3 and MCF-7 tumor cell lines, with doxorubicin (DOX) as the positive control. The results are shown in Table 3.

As shown in Table 3, most of the test compounds exhibited inhibitory activity against the tested tumor cell lines, indicating that the introduction of sulfonamide and dipeptide moiety on the DHAA skeleton markedly increased anti-tumor activity. Moreover, the antiproliferative activities of the tested compounds correlated well with their ability to inhibit MMP-3, with activities depending on the substituents at the R_1 position, and followed the order -CH_3> -H > -OCH_3> -Br> -F. Most of these compounds possessed methyl moiety in *meta*- or *para*-positions of the benzene ring which may have had certain steric electronic properties which enhanced lipophilicity and the ability to penetrate the cellular membrane leading to an increased antiproliferative effect. In addition, the activities of the sulfonamide derivatives **8** were better than those of the sulfoacid derivatives **9**. In this regard, compound **8k** with a methyl moiety at *meta*-positions of the benzene ring was the most potent compound, depending on the cell line tested, with IC_{50} values of 10.6±0.8, 4.2±1.1, 7.6±0.3 and 8.5±1.1 μM against NCI-H460, HepG2, SKOV-3 and MCF-7 cancer cells, respectively, and thus was more potent and effective than DHAA.

As the selectivity of antitumor agents for cancer cells over non-malignant cells is important to avoid numerous severe side effects, all compounds were tested using a non-cancerous liver cell line (HL-7702). As shown in Table 3, the cytotoxicity activities of most compounds against cancer cells was much higher than that against HL-7702 normal cells, making them good candidates as anticancer drugs. It was worth noting that all the DHAA derivatives demonstrated lower cytotoxicity on HL-7702 than the commercial anticancer drug DOX. These results showed that the targeted compounds had selective and significant effect on the cell lines.

*2.2.4. Compound **8k** inhibited the migration of HepG2 cell in vitro*

Metastasis plays an important role in later period of cancer progression. Thus, the inhibition of metastasis is vital for efficient cancer treatment. Migration of cells is a key attribute of practically

each biological process, particularly cancer cells where it is known to connect with the tumor progression and metastatic cascade [36]. As cell migration is connected with the metastatic activity of cancer cells, therefore we have investigated the effect of compound **8k** on HepG2 cells using wound healing assay. The migration of HepG2 cells was recorded by microscopic observations at 0 h, 24 h and 48 h after treatment with 5 μM and 10 μM of compound **8k**. Results from Fig. 3 clearly showed that there was almost complete healing of wound in control after 48 h, however healing was strongly suppressed in the cells treated with **8k**.

2.2.5 Cell cycle analysis

To determine the possible role of cell cycle arrest in **8k**-induced growth inhibition, HepG2 cells were treated with different concentrations of compound **8k**. Cell cycle distribution was investigated by flow cytometric analysis following staining of DNA with propidium iodide (PI). After treatment with compound **8k** at different concentrations for 24 h, it was observed that S phase cells gradually decreased and G2 phase cells did not change significantly, while G1 phase cells compared with the control cells gradually increased, respectively (Fig. 4). These results suggest that target compound **8k** mainly arrested HepG2 cells in the G1 phase.

*2.2.6 Compound **8k** induces apoptosis in HepG2 cells*

In order to confirm whether **8k**-induced reduction in cell viability was responsible for the induction of apoptosis, HepG2 cells were co-stained with PI and Annexin-V/FITC, and the number of apoptotic cells was estimated by flow cytometry (Fig. 5). Four quadrant images were observed by flow cytometry analysis: the Q1 area represented damaged cells which appeared during the process of cell collection, the Q2 region showed necrotic cells and later stage apoptotic cells; early apoptotic cells were located in the Q3 area and the Q4 area showed normal cells. A dose-dependent increase in the percentage of apoptotic cells was noted after the cells were treated with compound **8k** at the concentrations of 5 μM and 10 μM for 24 h. As shown in Fig. 5, few (5.07%) apoptotic cells were present in the control panel, in contrast, the percentage rose to 13.30% at the concentration of 5 μM after treatment with **8k** for 24 h. At concentrations of 10 μM, there was a further increase to 50.30% after treatment with **8k**. These results clearly confirmed that compared with the control, compound **8k** effectively induced apoptosis in HepG2 cells in a

dose-dependent manner.

2.2.7 Apoptosis assay by acridine orange/ethidium bromide (AO/EB) staining

To further characterize the cell apoptosis induced by compound **8k**, AO/EB staining was carried out to evaluate the accompanying changes in morphology. The cytotoxicity of compound **8k** was evaluated in HepG2 cells following treatment with 5 μM and 10 μM for 24 h. HepG2 cells not treated with **8k** were 24 h controls. The results (Fig. 6) showed that at both concentrations, the morphology of **8k**-treated HepG2 cells had changed significantly. The cell nuclei were stained yellow green or orange, and the morphology showed pycnosis, membrane blebbing and cell budding characteristic of apoptosis. The nearly complete absence of red-stained cells showed that **8k** treatment was associated with low toxicity. The results thus demonstrated that compound **8k** induced apoptosis with low toxicity.

3. Conclusion

A series of DHAA sulfonamide dipeptide derivatives were designed and synthesized as migration inhibitors which targeted MMPs with good IC_{50} values in low micromolar range. These compounds exhibited better inhibitory activities toward MMP-3 than MMP-8 and MMP-9, with IC_{50} values range from 0.4-59.7 μM. A docking study of the most active compound **8k** revealed key interactions between **8k** and MMP-3 in which the sulfonamide moiety and the dipeptide group was important for improving activity. It is noteworthy that further antitumor activity screening revealed that some compounds exhibited better inhibitory activity than the commercial anticancer drug 5-FU. In particular, compound **8k** (IC_{50} = 4.18 ± 1.08 μM) exhibited the best anticancer activity against the HepG2 cell line and displayed slightly weaker inhibitory activity than doxorubicin. The exposure of compound **8k** to HepG2 cells resulted in inhibition of *in vitro* cell migration through wound healing assay. The apoptosis-inducing activity investigated by flow cytometry revealed that compound **8k** markedly induced HepG2 cells apoptosis. The apoptosis inducing effect of **8k** was further analysed by AO/EB staining. In addition, cell cycle analysis indicated that compound **8k** arrested the HepG2 cell line in G1 phase. Consequently, the rational design of DHAA sulfonamide dipeptide derivatives offers significant potential for the discovery of a new class of MMPs inhibitors with the ability to suppress cancer cells migration. The precise

mechanism of this action requires further investigation.

4. Experimental

4.1 General information

Compound **3** was synthesized according to the literature [33]. Compound **6** was synthesized according to the literature [34]. All the chemical reagents and solvents used were of analytical grade. Silica gel (200-300 mesh) used in column chromatography was provided by Tsingtao Marine Chemistry Co. Ltd. ^{1}H NMR spectra were recorded on a BRUKER AV-400 spectrometer with TMS as an internal standard in $CDCl_3$. Mass spectra were determined on an FTMS ESI spectrometer.

*4.2. Synthesis: general procedure for compounds **8a-8u***

Compound **3** (1 mmol) added to dry CH_2Cl_2 (15 mL) and stirred at 0□. After that, oxalyl chloride (1.5 mmol) was dripped into the mixture and stirred at room temperature for 6 h. After the reaction, the solvent and excess oxalyl chloride was evaporated under reduced pressure. Aromatic primary amines (1 mmol) and triethylamine (0.5 mmol) were added to the mixture and stirred at room temperature for 0.5 h. After the reaction, the solvent was evaporated under reduced pressure, and the crude product was purified by chromatography on silica gel eluted with petroleum ether/ethylacetate (V:V = 6:1) to offer compound **4**. Compound **4** (1 mmol) and hydrazine hydrate (3 mmol) were added to ethanol (15 mL) and the mixture was stirred at room temperature for 8 h. After the reaction was completed, the solvent was evaporated under reduced pressure, and the crude product was purified by chromatography on silica gel eluted with petroleum ether/ethyl acetate (V: V = 3: 1) to obtain compounds **5**. Compounds **6** (1 mmol) added to dry H_2Cl_2 (15 mL) was stirred at 0 □ and oxalyl chloride (2.0 mmol) was dripped into the mixture and stirred at room temperature for 6 h. After the reaction, the solvent and excess oxalyl chloride was evaporated under reduced pressure. Compounds **5** (2 mmol) and triethylamine (1 mmol) were added to the mixture and stirred at room temperature for 18 h. After the reaction, the solvent was evaporated under reduced pressure, and the crude product was purified by chromatography on silica gel eluted with petroleum ether/ethyl acetate (V: V = 6:1) to offer compounds **8a-8u**. The structures were confirmed by ^{1}H NMR, ^{13}C NMR and HR-MS (see

Supporting information).

Compound **8a**: Yields 80.1%, as a white solid. Mp: 143.1−148.2 °C. $[\alpha]_D^{20}$ = +61 (*c* 0.1, AcOEt) ^{1}H NMR (400 MHz, $CDCl_3$) δ 8.94 (s, 1H), 7.81 (s, 1H), 7.72 (s, 1H), 7.29–7.26 (m, 3H), 7.21–7.15 (m, 8H), 7.14–7.10 (m, 2H), 7.08–7.03 (m, 2H), 6.99 (s, 1H), 6.89–6.79 (m, 4H), 6.63 (d, *J* = 7.3 Hz, 1H), 5.61 (d, *J* = 7.3 Hz, 1H), 4.95–4.89 (m, 1H), 4.22–4.17 (m, 1H), 3.66–3.60 (m, 1H), 3.25–3.12 (m, 2H), 3.10–3.04 (m, 1H), 2.98–2.93 (m, 1H), 2.73–2.67 (m, 1H), 2.58–2.51 (m, 1H), 2.19 (d, *J* = 12.4 Hz, 1H), 1.96 (d, *J* = 12.5 Hz, 1H), 1.73–1.58 (m, 3H), 1.41–1.31 (m, 3H), 1.26–1.20 (m, 6H, 2 × CH3), 1.17 (s, 3H, CH3), 1.00 (s, 3H, CH3). ^{13}C NMR (100 MHz, $CDCl_3$) δ 179.30, 169.68, 168.55, 159.59 (^1J(C,F) = 242.9 Hz), 159.29 (^1J(C,F) = 242.3 Hz), 147.47, 145.04, 141.26, 136.39, 135.46, 134.05, 133.67 (^4J(C,F) = 2.8 Hz), 132.87 (^4J(C,F) = 2.9 Hz), 129.32, 129.17, 128.95, 128.73, 127.42, 127.14, 125.14, 122.05 (^3J(C,F) = 7.9 Hz), 121.60 (^3J(C,F) = 7.8 Hz), 115.47 (^2J(C,F) = 22.3 Hz), 115.38 (^2J(C,F) = 22.3 Hz), 58.38, 55.40, 47.23, 45.00, 39.41, 38.04, 37.58, 37.06, 36.63, 29.71, 29.56, 29.35, 24.79, 24.28, 24.10, 20.46, 18.26, 16.29. HR-MS (*m*/*z*) (ESI): calcd for $C_{50}H_{54}F_2N_4NaO_5S$ $[M + Na]^+$: 883.3675; found: 883.3665.

Compound **8b**: Yields 87.5%, as a white solid. Mp: 148.8−152.1 °C. $[\alpha]_D^{20}$ = +56 (*c* 0.1, AcOEt) ^{1}H NMR (400 MHz, DMSO-d_6) δ 10.28 (s, 1H), 9.96 (s, 1H), 8.16 (d, *J* = 9.2 Hz, 1H), 7.90–7.88 (m, 1H), 7.62 (d, *J* = 7.6 Hz, 1H), 7.58 (s, 1H), 7.42–7.46 (m, 1H), 7.37 (d, *J* = 9.1 Hz, 1H), 7.35–7.31 (m, 1H), 7.28–7.17 (m, 11H), 7.05 (s, 1H), 7.01–6.97 (m, 1H), 4.69–4.57 (m, 1H), 4.17–4.11 (m, 1H), 3.81–3.59 (m, 1H), 3.04–2.81 (m, 4H), 2.62–2.55 (m, 1H), 2.46–2.39 (m, 1H), 2.08 (d, *J* = 11.8 Hz, 1H), 1.86–1.79 (m, 1H), 1.59 (s, 2H), 1.46 (s, 1H), 1.34–1.24 (m, 6H), 1.12–1.08 (m, 4H), 1.03 (s, 3H, CH_3), 0.78 (s, 3H, CH_3). ^{13}C NMR (100 MHz, DMSO-d_6) δ 177.61, 170.82, 168.96, 153.21 (^1J(C,F) = 241.5 Hz), 153.09 (^1J(C,F) = 241.2 Hz), 146.60, 144.41, 140.02, 137.90, 136.77, 136.14 (^4J(C,F) = 2.8 Hz), 135.65, 135.25 (^4J(C,F) = 3.0 Hz), 129.30, 129.02, 128.07, 127.97, 127.71, 126.50, 126.30, 124.15, 121.48, 120.51, 120.00 (^3J(C,F) = 7.1 Hz) , 119.43 (^3J(C,F) = 6.6 Hz), 119.12 (^2J(C,F) = 18.2 Hz), 118.72 (^2J(C,F) = 18.3 Hz), 116.96 (^2J(C,F) = 21.6 Hz), 116.53 (^2J(C,F) = 21.8 Hz), 58.11, 55.29, 46.23, 44.04, 38.56, 37.29, 36.73, 36.56, 35.92, 28.66, 28.22, 24.89, 23.67, 23.05, 19.77, 18.00, 16.13. HR-MS (*m*/*z*) (ESI): calcd for $C_{50}H_{52}Cl_2F_2N_4NaO_5S$ $[M + Na]^+$: 951.2895; found: 951.2883.

Compound **8c**: Yields 62.4%, as a white solid. Mp: 147.2−151.7 °C. $[\alpha]_D^{20}$= +65 (c 0.1, AcOEt) ^{1}H NMR (400 MHz, DMSO-d_6) δ 10.27 (s, 1H), 9.99 (s, 1H), 8.13 (d, *J* = 9.3 Hz, 1H), 7.65–7.54 (m, 3H), 7.35–7.32 (m, 1H), 7.29–7.18 (m, 12H), 7.16–7.10 (m, 1H), 7.04 (s, 1H), 6.93–6.78 (m, 3H), 4.74–4.56 (m, 1H), 4.23–4.14 (m, 1H), 3.71–3.66 (m, 1H), 3.10–2.92 (m, 3H), 2.89–2.84 (m, 1H), 2.58–2.51 (m, 1H), 2.44–2.35 (m, 1H), 2.08 (d, *J* = 11.8 Hz, 1H), 1.85–1.77 (m, 1H), 1.58 (s, 2H), 1.43 (s, 1H), 1.30–1.25 (m, 7H), 1.11 (d, *J* = 6.6 Hz, 3H, CH_3), 1.03 (s, 3H, CH_3), 0.81 (s, 3H, CH_3). ^{13}C NMR (100 MHz, DMSO-d_6) δ 177.59, 170.94, 169.15, 162.12 (^1J(C,F) = 240.0 Hz), 161.85 (^1J(C,F) = 239.6 Hz), 146.66, 144.28, 140.63 (^3J(C,F) = 10.9 Hz), 139.90 (^3J(C,F) = 9.7 Hz), 137.93, 136.80, 135.78, 130.39 (^3J(C,F) = 9.5 Hz), 129.96 (^3J(C,F) = 9.5 Hz), 129.31, 129.02, 128.04, 127.95, 127.73, 126.46, 126.29, 123.90, 115.35 (^4J(C,F) = 2.2 Hz), 114.88 (^4J(C,F) = 2.2 Hz), 109.84 (^2J(C,F) = 21.0 Hz), 109.73 (^2J(C,F) = 21.0 Hz), 106.54 (^2J(C,F) = 26.0 Hz), 105.92 (^2J(C,F) = 26.1 Hz), 58.14, 55.28, 46.22, 44.04, 38.76, 37.28, 36.75, 36.56, 35.94, 28.61, 28.22, 24.75, 23.75, 23.16, 19.76, 17.98, 16.12. HR-MS (*m*/*z*) (ESI): calcd for $C_{50}H_{54}F_2N_4NaO_5S$ [M + Na]$^+$: 883.3675; found: 883.3665.

Compound **8d**: Yields 51.6%, as a white solid. Mp: 155.4−158.9 °C. $[\alpha]_D^{20}$= +58 (*c* 0.1, AcOEt) ^{1}H NMR (400 MHz, DMSO-d_6) δ 10.25 (s, 1H), 9.93 (s, 1H), 8.16 (d, *J* = 9.3 Hz, 1H), 7.94 (s, 1H), 7.63 (d, *J* = 7.8 Hz, 1H), 7.59 (s, 1H), 7.47 (d, *J* = 7.8 Hz, 1H), 7.43 (s, 1H), 7.30–7.15 (m, 12H), 7.18–7.13 (m, 2H), 7.06–7.02 (m, 2H), 4.73–4.59 (m, 1H), 4.20–4.14 (m, 1H), 3.73–3.66 (m, 1H), 3.07–2.89 (m, 4H), 2.63–2.57 (m, 1H), 2.44–2.35 (m, 1H), 2.08 (d, *J* = 11.9 Hz, 1H), 1.82 (d, *J* = 13.6 Hz, 1H), 1.61 (d, *J* = 9.1 Hz, 2H), 1.46 (s, 1H), 1.36–1.23 (m, 7H), 1.12 (d, *J* = 6.6 Hz, 3H, CH_3), 1.03 (s, 3H CH_3), 0.78 (s, 3H, CH_3). ^{13}C NMR (100 MHz, DMSO-d_6) δ 177.62, 170.93, 169.05, 146.59, 144.31, 140.49, 140.02, 139.62, 137.94, 136.80, 135.62, 130.77, 130.28, 129.32, 129.02, 128.05, 127.95, 127.70, 126.48, 126.29, 126.03, 125.89, 124.11, 122.41, 121.54, 121.45, 121.12, 118.41, 117.90, 58.11, 55.34, 46.24, 44.05, 38.65, 37.29, 36.71, 36.57, 35.94, 28.71, 28.23, 24.92, 23.74, 23.06, 19.79, 18.01, 16.15. HR-MS (*m*/*z*) (ESI): calcd for $C_{50}H_{54}Br_2N_4NaO_5S$ [M + Na]$^+$: 1005.2053; found: 1005.2048.

Compound **8e**: Yields 52.4%, as a white solid. Mp: 155.6−158.4 °C. $[\alpha]_D^{20}$= +28 (*c* 0.1, AcOEt) ^{1}H

NMR (400 MHz, DMSO-d_6) δ 10.23 (s, 1H), 10.07 (s, 1H), 8.25 (d, *J* = 8.8 Hz, 1H), 7.93 (s, 1H), 7.79 (s, 1H), 7.70–7.61 (m, 2H), 7.53–7.49 (m, 1H), 7.33–7.24 (m, 6H), 7.22–7.15 (m, 9H), 7.03 (d, *J* = 14.4 Hz, 1H), 4.73–4.67 (m, 1H), 4.33–4.15 (m, 1H), 3.73–3.66 (m, 1H), 3.09–2.94 (m, 3H), 2.90–2.84 (m, 1H), 2.71–2.58 (m, 2H), 2.18 (d, *J* = 11.9 Hz, 1H), 1.88 (d, *J* = 13.3 Hz, 1H), 1.61–1.54 (m, 3H), 1.49–1.37 (m, 1H), 1.31–1.23 (m, 2H), 1.17 (d, *J* = 6.7 Hz, 3H, CH_3), 1.11 (d, *J* = 6.7 Hz, 3H, CH_3), 1.04 (s, 3H, CH_3), 0.97 (s, 3H, CH_3). ^{13}C NMR (100 MHz, DMSO-d_6) δ 177.37, 171.00, 169.36, 146.92, 143.81, 140.45, 139.78, 139.75, 137.85, 136.61, 136.50, 130.73, 130.48, 129.18, 129.13, 128.00, 127.95, 127.78, 126.41, 126.26, 126.12, 125.89, 123.34, 121.72, 121.52, 121.48, 121.30, 118.02, 117.98, 58.22, 55.32, 46.20, 46.17, 43.84, 38.90, 36.88, 36.67, 36.65, 35.67, 28.98, 28.07, 24.50, 24.06, 23.70, 19.65, 18.16, 16.21. HR-MS (*m*/*z*) (ESI): calcd for $C_{50}H_{54}Br_2N_4NaO_5S$ $[M + Na]^+$: 1005.2053; found: 1005.2044.

Compound **8f**: Yields 88.9%, as a white solid. Mp: 150.7−154.1 °C. $[\alpha]_D^{20}$ = +65 (*c* 0.1, AcOEt) ^{1}H NMR (400 MHz, $CDCl_3$) δ 8.53 (s, 1H), 7.78 (s, 1H), 7.65 (s, 1H), 7.40 (d, *J* = 7.7 Hz, 2H), 7.30–7.24 (m, 15H), 7.09 (t, *J* = 7.0 Hz, 4H), 7.04 (s, 1H), 6.60 (d, *J* = 7.6 Hz, 1H), 5.57 (d, *J* = 7.3 Hz, 1H), 4.91–4.97 (m, 1H), 4.16–4.13 (m, 1H), 3.72–3.63 (m, 1H), 3.24–3.16 (m, 3H), 3.04–2.99 (m, 1H), 2.70 (t, *J* = 15.8 Hz, 2H), 2.27 (d, *J* = 12.2 Hz, 1H), 1.97 (d, *J* = 11.8 Hz, 1H), 1.90 (s, 1H), 1.65–1.43 (m, 5H), 1.25 (d, *J* = 6.7 Hz, 6H, 2 × CH_3), 1.19 (s, 3H, CH_3), 1.10 (s, 3H, CH_3). ^{13}C NMR (100 MHz, $CDCl_3$) δ 179.19, 169.71, 168.35, 147.66, 145.03, 141.45, 137.59, 136.90, 136.83, 135.73, 134.07, 129.45, 129.42, 129.07, 129.03, 128.88, 127.53, 127.22, 125.37, 124.94, 124.61, 120.29, 120.17, 58.63, 55.58, 47.30, 44.76, 39.58, 37.98, 37.50, 37.21, 36.91, 29.82, 29.41, 25.11, 24.47, 24.15, 20.36, 18.40, 16.46. HR-MS (*m*/*z*) (ESI): calcd for $C_{50}H_{56}N_4NaO_5S$ $[M + Na]^+$: 847.3863; found: 847.3857.

Compound **8g**: Yields 85.7%, as a white solid. Mp: 151.2−154.6 °C. $[\alpha]_D^{20}$ = +37 (*c* 0.1, AcOEt) ^{1}H NMR (400 MHz, $CDCl_3$) δ 8.68 (s, 1H), 7.74 (d, *J* = 1.8 Hz, 2H), 7.36 (d, *J* = 7.7 Hz, 2H), 7.28–7.17 (m, 15H), 7.09–7.03 (m, 4H), 6.99 (s, 1H), 6.65 (d, *J* = 7.7 Hz, 1H), 5.67 (d, *J* = 7.4 Hz, 1H), 4.99–4.94 (m, 1H), 4.16–4.11 (m, 1H), 3.67–3.58 (m, 1H), 3.22–3.12 (m, 3H), 3.01–2.96 (m, 1H), 2.71–2.53 (m, 2H), 2.21 (d, *J* = 12.1 Hz, 1H), 2.03 (s, 1H), 1.94 (d, *J* = 12.4 Hz, 1H), 1.61–1.39 (m, 5H), 1.20 (d, *J* = 6.7 Hz, 6H, 2 × CH_3), 1.15 (s, 3H, CH_3), 1.04 (s, 3H, CH_3). ^{13}C

NMR (100 MHz, $CDCl_3$) δ 179.19, 169.85, 168.41, 147.60, 144.96, 141.39, 137.59, 136.90, 136.79, 135.70, 134.09, 129.42, 129.40, 128.98, 128.80, 127.46, 127.15, 125.26, 124.89, 124.56, 120.29, 120.17, 58.61, 55.54, 47.25, 44.68, 39.57, 38.05, 37.42, 37.17, 36.86, 29.79, 29.36, 25.10, 24.48, 24.09, 20.32, 18.35, 16.44. HR-MS (*m*/*z*) (ESI): calcd for $C_{50}H_{56}N_4NaO_5S$ $[M + Na]^+$: 847.3863; found: 847.3857.

Compound **8h**: Yields 76.3%, as a white solid. Mp: 128.6−133.7 °C. $[\alpha]_D^{20}$ = +62 (*c* 0.1, AcOEt) ^1H NMR (400 MHz, $CDCl_3$) δ 8.74 (s, 1H), 7.74 (s, 1H), 7.65 (s, 1H), 7.29–7.19 (m, 9H), 7.16 (s, 1H), 7.13–7.09 (m, 3H), 7.07 (d, *J* = 6.8 Hz, 1H), 7.01 (s, 1H), 6.92 (s, 1H), 6.85 (d, *J* = 8.0 Hz, 1H), 6.67 (d, *J* = 8.1 Hz, 1H), 6.63–6.61 (m, 3H), 5.56 (d, *J* = 7.6 Hz, 1H), 4.97–4.88 (m, 1H), 4.28–4.18 (m, 1H), 3.74 (s, 6H, 2 × OCH_3), 3.69–3.69 (m, 1H), 3.26–3.17 (m, 2H), 3.15–3.09 (m, 1H), 3.02–2.97 (m, 1H), 2.74–2.68 (m, 1H), 2.65–2.58 (m, 1H), 2.23 (d, *J* = 13.3 Hz, 1H), 2.00 (d, *J* = 12.6 Hz, 1H), 1.93 (s, 1H), 1.68–1.56 (m, 3H), 1.36 (d, *J* = 11.8 Hz, 2H), 1.28–1.23 (m, 6H, 2 × CH_3), 1.19 (s, 3H, CH_3), 1.01 (s, 3H, CH_3). ^{13}C NMR (100 MHz, $CDCl_3$) δ 179.27, 169.43, 168.33, 160.24, 160.14, 147.72, 145.04, 141.59, 138.75, 138.02, 136.60, 135.59, 133.97, 129.76, 129.69, 129.49, 129.37, 129.23, 128.98, 128.88, 127.66, 127.34, 125.42, 112.43, 112.23, 110.70, 110.52, 106.08, 105.75, 58.65, 55.43, 47.37, 45.08, 39.50, 37.80, 37.73, 37.21, 36.91, 29.66, 29.54, 24.84, 24.41, 24.30, 20.69, 18.39, 16.42. HR-MS (*m*/*z*) (ESI): calcd for $C_{52}H_{60}N_4NaO_7S$ $[M + Na]^+$: 907.4074; found: 907.4067.

Compound **8i**: Yields 79.8%, as a white solid. Mp: 129.1−134.2 °C. $[\alpha]_D^{20}$ = +44 (*c* 0.1, AcOEt) ^1H NMR (400 MHz, $CDCl_3$) δ 8.51 (s, 1H), 7.71 (s, 1H), 7.58 (s, 1H), 7.25–7.16 (m, 9H), 7.10–7.01 (m, 5H), 6.98 (s, 1H), 6.93 (t, *J* = 2.1 Hz, 1H), 6.83 (d, *J* = 8.0 Hz, 1H), 6.65 (d, *J* = 8.0 Hz, 1H), 6.59–6.56 (m, 2H), 6.53 (d, *J* = 7.6 Hz, 1H), 5.46 (d, *J* = 7.2 Hz, 1H), 4.90–4.84 (m, 1H), 4.09–4.04 (m, 1H), 3.69 (d, *J* = 1.0 Hz, 6H, 2 × OCH_3), 3.62–3.53 (m, 1H), 3.22–3.05 (m, 3H), 2.97–2.91 (m, 1H), 2.68–2.56 (m, 2H), 2.19 (d, *J* = 12.3 Hz, 1H), 1.89–1.83 (m, 2H), 1.48–1.41 (m, 3H), 1.30–1.21 (m, 2H), 1.19–1.16 (m, 6H, 2 × CH_3), 1.12 (s, 3H, CH_3), 1.04 (s, 3H, CH_3). ^{13}C NMR (100 MHz, $CDCl_3$) δ 179.23, 169.74, 168.32, 160.17, 160.09, 147.68, 145.02, 141.47, 138.82, 138.10, 136.84, 135.68, 134.04, 129.70, 129.42, 129.38, 129.07, 128.87, 127.52, 127.19, 125.41, 112.44, 112.34, 110.87, 110.43, 105.93, 105.85, 58.64, 55.64, 55.39, 55.36, 47.31, 44.85,

39.50, 37.88, 37.47, 37.23, 36.86, 29.82, 29.40, 25.12, 24.50, 24.11, 20.32, 18.42, 16.45. HR-MS (*m*/*z*) (ESI): calcd for $C_{52}H_{60}N_4NaO_7S$ $[M + Na]^+$: 907.4074; found:907.4068.

Compound **8j**: Yields 76.8%, as a white solid. Mp: 135.8−139.2 °C. $[\alpha]_D^{20}$ = +63 (*c* 0.1, AcOEt) ^1H NMR (400 MHz, $CDCl_3$) δ 8.55 (s, 1H), 7.64 (s, 1H), 7.51 (s, 1H), 7.24–7.18 (m, 10H), 7.11–7.02 (m, 6H), 6.98–6.95 (m, 2H), 6.78 (t, *J* = 7.2 Hz, 2H), 6.53 (d, *J* = 7.4 Hz, 1H), 5.43 (d, *J* = 7.5 Hz, 1H), 4.98–4.88 (m, 1H), 4.20–4.15 (m, 1H), 3.67–3.61 (m, 1H), 3.24–3.08 (m, 3H), 3.00–2.94 (m, 1H), 2.66–2.42 (m, 2H), 2.15 (d, *J* = 6.8 Hz, 6H, 2 × CH_3), 1.92 (d, *J* = 11.5 Hz, 1H), 1.66–1.53 (m, 5H), 1.41–1.34 (m, 2H), 1.26–1.22 (m, 6H, 2 × CH_3), 1.09 (s, 3H, CH_3), 0.93 (s, 3H, CH_3). ^{13}C NMR (100 MHz, $CDCl_3$) δ 179.11, 169.56, 168.28, 147.52, 144.89, 141.32, 138.78, 138.73, 137.47, 136.72, 136.50, 135.55, 134.05, 129.41, 129.27, 129.00, 128.73, 128.66, 127.43, 127.11, 125.57, 125.20, 125.15, 120.83, 120.63, 117.27, 117.10, 58.49, 55.30, 47.24, 45.00, 39.53, 37.95, 37.60, 37.08, 36.65, 29.73, 29.60, 29.37, 24.78, 24.23, 21.42, 20.48, 18.25, 16.31. HR-MS (*m*/*z*) (ESI): calcd for $C_{52}H_{61}N_4O_5S$ $[M + H]^+$: 853.4357; found:853.4363.

Compound **8k**: Yields 78.9%, as a white solid. Mp: 136.6−139.8 °C. $[\alpha]_D^{20}$ = +36 (*c* 0.1, AcOEt) ^1H NMR (400 MHz, $CDCl_3$) δ 8.62 (s, 1H), 7.74 (s, 1H), 7.66 (s, 1H), 7.24–7.20 (m, 10H), 7.16–7.07 (m, 6H), 6.99 (d, *J* = 8.5 Hz, 2H), 6.87 (t, *J* = 6.3 Hz, 2H), 6.63 (s, 1H), 5.68–5.56 (m, 1H), 5.02–4.89 (m, 1H), 4.11 (d, *J* = 3.9 Hz, 1H), 3.64–3.61 (m, 1H), 3.23–3.13 (m, 3H), 3.01–2.95 (m, 1H), 2.66 (d, *J* = 6.3 Hz, 2H), 2.25 (d, *J* = 7.4 Hz, 6H, 2 × CH_3), 2.04–1.94 (m, 2H), 1.57–1.42 (m, 6H), 1.20 (d, *J* = 5.4 Hz, 6H, 2 × CH_3), 1.16 (s, 3H, CH_3), 1.06 (s, 3H, CH_3). ^{13}C NMR (100 MHz, $CDCl_3$) δ 179.11, 169.71, 168.24, 147.55, 144.87, 141.30, 138.81, 138.77, 137.43, 136.78, 136.75, 135.63, 134.01, 129.35, 129.33, 128.94, 128.73, 128.71, 127.38, 127.06, 125.63, 125.27, 120.78, 120.69, 117.25, 117.15, 58.52, 55.51, 47.18, 44.64, 39.48, 37.94, 37.40, 37.11, 36.80, 29.73, 29.28, 25.05, 24.50, 23.96, 21.43, 20.26, 18.30, 16.41. HR-MS (*m*/*z*) (ESI): calcd for $C_{52}H_{61}N_4O_5S$ $[M + H]^+$: 853.4357; found:853.4363.

Compound **8l**: Yields 81.4%, as a white solid. Mp: 135.9−140.1°C. $[\alpha]_D^{20}$ = +67 (*c* 0.1, AcOEt) ^1H NMR (400 MHz, $CDCl_3$) δ 8.32–8.29 (m, 1H), 8.16–8.14 (m, 1H), 8.00 (s, 1H), 7.83 (s, 1H), 7.70 (s, 1H), 7.35–7.18 (m, 9H), 7.12–7.09 (m, 2H), 7.07–6.99 (m, 3H), 6.97–6.88 (m, 2H), 6.84–6.82

(m, 1H), 6.79–6.74 (m, 1H), 6.48 (d, *J* = 7.3 Hz, 1H), 5.43 (d, *J* = 7.5 Hz, 1H), 4.88–4.79 (m, 1H), 4.15–4.10 (m, 1H), 3.73 (s, 3H, OCH_3), 3.67 (s, 3H, OCH_3), 3.66–3.61 (m, 1H), 3.27–3.22 (m, 1H), 3.14 (d, *J* = 7.1 Hz, 2H), 2.98–2.93 (m, 1H), 2.71 (t, *J* = 8.3 Hz, 2H), 2.27 (d, *J* = 12.1 Hz, 1H), 2.04–2.00 (m, 1H), 1.68–1.60 (m, 5H), 1.51 (d, *J* = 6.3 Hz, 1H), 1.38 (d, *J* = 15.4 Hz, 2H), 1.28 (d, *J* = 6.7 Hz, 3H, CH_3), 1.23 (d, *J* = 6.7 Hz, 3H, CH_3), 1.20 (s, 3H, CH_3), 1.05 (s, 3H, CH_3). ^{13}C NMR (100 MHz, $CDCl_3$) δ 178.30, 169.13, 167.96, 148.13, 148.08, 147.58, 145.04, 141.26, 136.56, 135.63, 134.29, 129.49, 129.40, 129.01, 128.82, 128.74, 127.37, 127.16, 127.09, 126.74, 124.96, 124.41, 124.27, 121.11, 120.98, 119.90, 119.84, 110.09, 110.06, 58.98, 55.72, 55.71, 55.42, 47.26, 44.93, 40.19, 38.63, 37.77, 37.20, 37.17, 29.69, 29.58, 24.70, 24.33, 24.30, 20.71, 18.43, 16.51. HR-MS (*m*/*z*) (ESI): calcd for $C_{52}H_{60}KN_4O_7S$ $[M + K]^+$: 923.3814; found: 923.3816.

Compound **8m**: Yields 82.4%, as a white solid. Mp: 136.8−140.4 °C. $[\alpha]_D^{20}$ = +32 (*c* 0.1, AcOEt) ^{1}H NMR (400 MHz, $CDCl_3$) δ 8.60 (s, 1H), 7.77 (s, 1H), 7.72 (s, 1H), 7.28–7.22 (m, 11H), 7.13–7.09 (m, 4H), 7.03 (s, 1H), 6.82–6.70 (m, 5H), 5.72 (d, *J* = 7.5 Hz, 1H), 5.00–4.95 (m, 1H), 4.17–4.12 (m, 1H), 3.76 (s, 6H, 2 × OCH_3), 3.76–3.61 (m, 1H), 3.25–3.12 (m, 3H), 3.03–2.98 (m, 1H), 2.69–2.65 (m, 2H), 2.23 (d, *J* = 13.7 Hz, 2H), 1.98 (d, *J* = 12.5 Hz, 1H), 1.58–1.46 (m, 5H), 1.24–1.21 (m, 6H, 2 × CH_3), 1.18 (s, 3H, CH_3), 1.07 (s, 3H, CH_3). ^{13}C NMR (100 MHz, $CDCl_3$) δ 178.97, 169.54, 168.18, 156.72, 156.50, 147.53, 144.91, 141.32, 136.83, 135.73, 134.04, 130.57, 129.88, 129.39, 129.37, 128.89, 128.71, 127.35, 127.05, 125.22, 122.13, 121.92, 114.07, 114.05, 58.40, 55.47, 55.33, 47.15, 44.58, 39.57, 38.12, 37.35, 37.08, 36.77, 29.76, 29.28, 25.03, 24.38, 24.06, 20.27, 18.30, 16.38. HR-MS (*m*/*z*) (ESI): calcd for $C_{52}H_{60}KN_4O_7S$ $[M + K]^+$: 923.3814; found: 923.3810.

Compound **8n**: Yields 79.5%, as a white solid. Mp: 139.0−144.6 °C. $[\alpha]_D^{20}$ = +59 (*c* 0.1, AcOEt) ^{1}H NMR (400 MHz, $CDCl_3$) δ 8.76 (s, 1H), 7.71 (s, 2H), 7.34–7.12 (m, 11H), 7.11–7.06 (m, 2H), 7.03 (d, *J* = 8.5 Hz, 2H), 6.96 (t, *J* = 8.6 Hz, 5H), 6.69 (d, *J* = 7.0 Hz, 1H), 5.80–5.56 (m, 1H), 5.02–4.85 (m, 1H), 4.25–4.11 (m, 1H), 3.74–3.59 (m, 1H), 3.12 (m, 3H), 2.98 (m, 1H), 2.71–2.50 (m, 2H), 2.26 (s, 6H, 2 × CH_3), 2.18 (d, *J* = 11.3 Hz, 1H), 1.96 (d, *J* = 16 Hz, 1H), 1.67–1.46 (m, 4H), 1.39–1.29 (m, 2H), 1.24–1.20 (m, 6H, 2 × CH_3), 1.14 (s, 3H, CH_3), 0.97 (s, 3H, CH_3). ^{13}C NMR (100 MHz, $CDCl_3$) δ 179.16, 169.76, 168.40, 147.55, 144.93, 141.31, 136.65, 135.73,

135.09, 134.44, 134.37, 134.32, 134.02, 129.49, 129.36, 128.95, 128.72, 127.40, 127.09, 125.09, 120.39, 120.17, 58.51, 55.40, 47.26, 45.03, 39.80, 38.18, 37.60, 37.13, 36.67, 29.66, 29.38, 24.84, 24.35, 24.23, 20.95, 20.51, 18.32, 16.35. HR-MS (*m*/*z*) (ESI): calcd for $C_{52}H_{61}N_4O_5S$ $[M + H]^+$: 853.4357; found:853.4360.

Compound **8o**: Yields 75.2%, as a white solid. Mp: 139.7−145.3 °C. $[\alpha]_D^{20}$ = +35 (*c* 0.1, AcOEt) ^{1}H NMR (400 MHz, $CDCl_3$) δ 8.11 (s, 1H), 7.79 (s, 1H), 7.40 (s, 1H), 7.36–7.20 (m, 11H), 7.14–7.04 (m, 9H), 6.52 (d, *J* = 7.4 Hz, 1H), 5.39 (d, *J* = 7.1 Hz, 1H), 4.86–4.80 (m, 1H), 4.08–4.03 (m, 1H), 3.70–3.59 (m, 1H), 3.29–3.24 (m, 1H), 3.22–3.13 (m, 2H), 3.00–2.94 (m , 1H), 2.78–2.65 (m, 2H), 2.31 (d, *J* = 2.7 Hz, 6H, 2 × CH_3), 2.03–2.00 (m, 1H), 1.73–1.68 (m, 4H), 1.60–1.49 (m, 2H), 1.41–1.32 (m, 1H), 1.25 (m, 6H, 2 × CH_3), 1.20 (s, 3H, CH_3), 1.14 (s, 3H, CH_3). ^{13}C NMR (100 MHz, $CDCl_3$) δ 179.08, 169.30, 168.05, 147.69, 145.03, 141.53, 136.93, 135.75, 134.91, 134.67, 134.32, 134.24, 133.84, 129.57, 129.56, 129.48, 129.43, 129.14, 128.97, 128.85, 127.59, 127.27, 125.56, 120.32, 120.16, 58.51, 55.62, 47.32, 44.75, 39.59, 37.85, 37.56, 37.22, 36.88, 29.86, 29.43, 25.13, 24.52, 24.18, 21.02, 21.00, 20.34, 18.44, 16.44. HR-MS (*m*/*z*) (ESI): calcd for $C_{52}H_{61}N_4O_5S$ $[M + H]^+$: 853.4357; found:853.4365.

Compound **8p**: Yields 69.4%, as a white solid. Mp: 122.4−126.8 °C. $[\alpha]_D^{20}$ = +68 (*c* 0.1, AcOEt) ^{1}H NMR (400 MHz, $CDCl_3$) δ 8.49 (d, *J* = 11.9 Hz, 1H), 8.22 (d, *J* = 8.3 Hz, 1H), 8.09 (s, 1H), 7.77 (d, *J* = 6.1 Hz, 2H), 7.28 (m, 9H), 7.17–6.94 (m, 9H), 6.46 (d, *J* = 7.2 Hz, 1H), 5.48–5.30 (m, 1H), 5.03–4.87 (m, 1H), 4.23–4.13 (m, 1H), 3.71–3.57 (m, 1H), 3.29–3.14 (m, 3H), 3.07–2.95 (m, 1H), 2.72 (s, 2H), 2.30 (d, *J* = 10.8 Hz, 1H), 2.09 (d, *J* = 9.0 Hz, 1H), 1.64 (d, *J* = 12.1 Hz, 3H), 1.38 (s, 3H), 1.31–1.22 (m, 6H, 2 × CH_3), 1.20 (d, *J* = 5.9 Hz, 3H, CH_3), 1.07 (s, 3H, CH_3). ^{13}C NMR (100 MHz, $CDCl_3$) δ 179.12, 169.73, 168.57, 152.68 (^1J(C,F) = 243.2 Hz), 152.61 (^1J(C,F) = 242.5 Hz), 147.51, 144.88, 141.52, 136.31, 135.15, 133.64, 129.23, 129.20, 129.08, 128.84, 128.70, 127.54, 127.22, 125.87 (^2J(C,F) = 10.3 Hz), 125.33 (^3J(C,F) = 8.4 Hz), 124.61 (^3J(C,F) = 7.5 Hz), 124.86, 124.78, 124.50 (^3J(C,F) = 3.5 Hz), 124.42 (^3J(C,F) = 3.3 Hz), 122.06, 121.97, 114.97 (^2J(C,F) = 19.4 Hz), 114.92 (^2J(C,F) = 19.2 Hz), 58.61, 55.08, 47.25, 44.74, 39.29, 37.61, 37.37, 37.04, 36.86, 29.84, 29.45, 24.70, 24.32, 24.12, 20.64, 18.30, 16.33. HR-MS (*m*/*z*) (ESI): calcd for $C_{50}H_{54}F_2KN_4O_5S$ $[M + K]^+$: 899.3414; found: 899.3409.

Compound **8q**: Yields 73.3%, as a white solid. Mp: 122.3−126.5 °C. $[\alpha]_D^{20}$ = +29 (*c* 0.1, AcOEt) ^{1}H NMR (400 MHz, $CDCl_3$) δ 8.41 (s, 1H), 8.13 (t, *J* = 7.8 Hz, 1H), 7.96 (t, *J* = 7.8 Hz, 1H), 7.69 (s, 1H), 7.63–7.60 (m, 1H), 7.27–7.12 (m, 8H), 7.06–6.94 (m, 9H), 6.40–6.31 (m, 1H), 5.38–5.31 (m, 1H), 4.89–4.32 (m, 1H), 4.09–4.04 (m, 1H), 3.56–3.51 (m, 1H), 3.24–3.01 (m, 3H), 2.98–2.92 (m, 1H), 2.70–2.50 (m, 2H), 2.17 (d, *J* = 12.6 Hz, 1H), 1.87–1.84 (m, 2H), 1.65–1.35 (m, 5H), 1.19–1.09 (m, 9H, 3 × CH_3), 1.04 (s, 3H, CH_3). ^{13}C NMR (100 MHz, $CDCl_3$) δ 179.12, 169.75, 168.42, 152.72 (^1J(C,F) = 243.5 Hz), 152.52 (^1J(C,F) = 243.6 Hz), 147.50, 144.88, 141.43, 136.55, 135.20, 133.67, 129.23, 129.20, 129.04, 128.88, 128.78, 128.69, 127.54, 127.21, 125.87 (^2J(C,F) = 10.5 Hz), 125.83 (^2J(C,F) = 10.6 Hz), 125.33 (^3J(C,F) = 7.2 Hz), 125.17 (^3J(C,F) = 7.4 Hz), 124.88, 124.81, 124.48 (^3J(C,F) = 3.1 Hz), 124.45 (^3J(C,F) = 2.9 Hz), 122.04, 121.85, 115.00 (^2J(C,F) = 19.0 Hz), 58.63, 55.34, 47.23, 44.42, 39.36, 37.27, 37.07, 37.04, 36.69, 29.74, 29.39, 25.04, 24.21, 24.18, 20.16, 18.30, 16.29. HR-MS (*m*/*z*) (ESI): calcd for $C_{50}H_{54}F_2KN_4O_5S$ $[M + K]^+$: 899.3414; found: 899.3408.

Compound **8r**: Yields 83.6%, as a white solid. Mp: 120.0−125.1 °C. $[\alpha]_D^{20}$ = +60 (*c* 0.1, AcOEt) ^{1}H NMR (400 MHz, $CDCl_3$) δ 8.63 (s, 1H), 7.71 (s, 1H), 7.61 (s, 1H), 7.27–7.15 (m, 11H), 7.09 (d, *J* = 6.4 Hz, 2H), 7.04 (d, *J* = 8.8 Hz, 2H), 6.98 (s, 1H), 6.75–6.65 (m, 5H), 5.62 (d, *J* = 7.7 Hz, 1H), 4.94–4.88 (m, 1H), 4.21–4.16 (m, 1H), 3.73 (s, 6H, 2 × OCH_3), 3.73–3.61 (m, 1H), 3.22–3.07 (m, 3H), 3.00–2.94 (m, 1H), 2.71–2.65 (m, 1H), 2.61–2.54 (m, 1H), 2.19 (d, *J* = 12.5 Hz, 1H), 1.97 (d, *J* = 9.1 Hz, 2H), 1.65–1.57 (m, 3H), 1.38–1.33 (m, 2H), 1.25–1.19 (m, 6H, 2 × CH_3), 1.16 (s, 3H, CH_3), 1.00 (s, 3H, CH_3). ^{13}C NMR (100 MHz, $CDCl_3$) δ 179.10, 169.51, 168.29, 156.78, 156.48, 147.55, 144.99, 141.30, 136.65, 135.73, 134.26, 130.75, 129.97, 129.52, 129.36, 128.98, 128.75, 127.43, 127.13, 125.12, 122.14, 121.82, 114.08, 114.04, 58.44, 55.57, 55.54, 55.31, 47.28, 45.03, 39.74, 38.25, 37.61, 37.15, 36.70, 29.67, 29.41, 24.90, 24.30, 24.28, 20.56, 18.35, 16.38. HR-MS (*m*/*z*) (ESI): calcd for $C_{52}H_{60}KN_4O_7S$ $[M + K]^+$: 923.3814; found:923.3820.

Compound **8s**: Yields 82.4%, as a white solid. Mp: 120.2−125.4 °C. $[\alpha]_D^{20}$ = +29 (*c* 0.1, AcOEt) ^{1}H NMR (400 MHz, $CDCl_3$) δ 8.22 (d, *J* = 8.0 Hz, 1H), 8.10 (s, 1H), 8.07 (d, *J* = 8.0 Hz, 1H), 7.74 (s, 1H), 7.64 (s, 1H), 7.20–7.11 (m, 8H), 7.02–7.00 (m, 2H), 6.96–6.89 (m, 3H), 6.86–6.79 (m, 2H),

6.74–6.68 (m, 2H), 6.39 (d, *J* = 7.6 Hz, 1H), 5.48 (d, *J* = 7.2 Hz, 1H), 4.82–4.77 (m, 1H), 4.05–4.00 (m, 1H), 3.64 (s, 3H, OCH_3), 3.56–3.51 (m, 4H), 3.14–3.08 (m, 3H), 3.06–3.03 (m, 1H), 2.93–2.88 (m, 2H), 2.16 (d, *J* = 12.8 Hz, 1H), 1.86–1.79 (m, 2H), 1.57–1.38 (m, 5H), 1.17–1.12 (m, 6H, 2 × CH_3), 1.08 (s, 3H, CH_3), 0.98 (s, 3H, CH_3). ^{13}C NMR (100 MHz, $CDCl_3$) δ 178.32, 169.21, 167.89, 148.11, 148.01, 147.41, 144.84, 141.17, 136.78, 135.62, 134.15, 129.33, 128.86, 128.76, 128.65, 127.24, 127.08, 127.03, 126.62, 125.10, 124.37, 124.19, 120.97, 120.90, 119.82, 119.78, 110.10, 110.07, 58.92, 55.64, 55.44, 47.16, 44.59, 39.95, 38.16, 37.29, 37.10, 36.78, 29.79, 29.40, 25.04, 24.22, 24.04, 20.23, 18.40, 16.40. HR-MS (*m*/*z*) (ESI): calcd for $C_{52}H_{60}KN_4O_7S$ [M + K]$^+$: 923.3814; found: 923.3815.

Compound **8t**: Yields 76.7%, as a white solid. Mp: 121.1−124.6 °C. $[\alpha]_D^{20}$ = +63 (*c* 0.1, AcOEt) ^{1}H NMR (400 MHz, $CDCl_3$) δ 7.99 (s, 1H), 7.85 (d, *J* = 7.9 Hz, 1H), 7.77 (s, 1H), 7.60 (d, *J* = 7.9 Hz, 1H), 7.48 (s, 1H), 7.37–7.27 (m, 5H), 7.25–7.22 (m, 3H), 7.20–7.02 (m, 10H), 6.39 (d, *J* = 7.3 Hz, 1H), 5.24 (d, *J* = 7.1 Hz, 1H), 4.87–4.81 (m, 1H), 4.12–4.07 (m, 1H), 3.60 (m, 1H), 3.33–3.12 (m, 3H), 2.96–2.91 (m, 1H), 2.70 (t, *J* = 8.6 Hz, 2H), 2.28 (d, *J* = 12.5 Hz, 1H), 2.07 (s, 3H, CH_3), 1.93 (d, *J* = 10.1 Hz, 4H), 1.49–1.46 (m, 2H), 1.29–1.26 (m, 4H), 1.25–1.22 (m, 6H, 2 × CH_3), 1.17 (s, 3H, CH_3), 1.13 (s, 3H, CH_3). ^{13}C NMR (100 MHz, $CDCl_3$) δ 179.19, 169.43, 168.39, 147.73, 145.02, 141.61, 137.01, 135.69, 135.54, 134.93, 133.72, 130.59, 130.55, 129.42, 129.37, 129.30, 129.22, 129.07, 128.82, 128.68, 127.66, 127.32, 126.79, 126.77, 125.67, 125.61, 125.15, 122.77, 122.29, 58.56, 55.65, 47.33, 44.81, 39.13, 37.51, 37.35, 37.19, 36.74, 29.83, 29.54, 25.11, 24.67, 24.05, 20.16, 18.42, 17.77, 17.37, 16.37. HR-MS (*m*/*z*) (ESI): calcd for $C_{52}H_{60}N_4NaO_5S$ [M + Na]$^+$: 875.4176; found: 875.4171.

Compound **8u**: Yields 74.5%, as a white solid. Mp: 120.9−124.3 °C. $[\alpha]_D^{20}$ = +31 (*c* 0.1, AcOEt) ^{1}H NMR (400 MHz, $CDCl_3$) δ 8.08 (s, 1H), 7.84 (d, *J* = 8.0 Hz, 1H), 7.79 (s, 1H), 7.60 (d, *J* = 8.0 Hz, 1H), 7.56 (s, 1H), 7.36–7.24 (m, 9H), 7.20–7.07 (m, 9H), 6.47 (d, *J* = 7.3 Hz, 1H), 5.36 (d, *J* = 7.1 Hz, 1H), 5.00–4.80 (m, 1H), 4.17–4.12 (m, 1H), 3.66–3.60 (m, 1H), 3.32–3.16 (m, 3H), 3.01–2.92 (m, 1H), 2.73 (t, *J* = 8.6 Hz, 2H), 2.30 (d, *J* = 12.7 Hz, 1H), 2.09 (s, 3H, CH_3), 1.95 (s, 3H, CH_3), 1.74–1.61 (m, 3H), 1.52–1.45 (m, 2H), 1.37 (s, 2H), 1.27–1.27 (m, 6H, 2 × CH_3), 1.19 (s, 3H, CH_3), 1.15 (s, 3H, CH_3). ^{13}C NMR (100 MHz, $CDCl_3$) δ 179.17, 169.53, 168.45, 147.71, 145.01,

141.57, 137.00, 135.65, 135.58, 134.93, 133.80, 130.58, 130.53, 129.43, 129.36, 129.16, 129.01, 128.89, 128.80, 127.60, 127.27, 126.73, 125.61, 125.21, 122.85, 122.46, 58.56, 55.61, 47.31, 44.79, 39.12, 37.49, 37.42, 37.18, 36.75, 29.84, 29.50, 25.09, 24.66, 24.01, 20.17, 18.41, 17.75, 17.36, 16.36. HR-MS (*m*/*z*) (ESI): calcd for $C_{52}H_{60}N_4NaO_5S$ $[M + Na]^+$: 875.4176; found: 875.4171.

*4.3. Synthesis: general procedure for compounds **9a-9i***

Compounds **5** (1 mmol) and triethylamine (0.5 mmol) were added to the mixture and stirred at room temperature for 2 h. After the reaction, the solvent was evaporated under reduced pressure, and the crude product was purified by chromatography on silica gel eluted with petroleum ether/ethyl acetate (V : V = 6:1) to offer compounds **9a-9i**. The structures were confirmed by ^{1}H NMR, ^{13}C NMR and HR-MS (see Supporting information).

Compound **9a**: Yields 61.8%, as a white solid. Mp: 164.8−169.7 °C. $[\alpha]_D^{20}$ = +43 (*c* 0.1, AcOEt) ^{1}H NMR (400 MHz, $CDCl_3$) δ 9.18 (s, 1H), 7.87 (s, 1H), 7.33 (d, *J* = 10.6 Hz, 1H), 7.28–7.25 (m, 3H), 7.20–7.16 (m, 2H), 7.13 (s, 1H), 7.03–6.97 (m, 2H), 6.70 (t, *J* = 7.6 Hz, 1H), 6.62 (d, *J* = 7.0 Hz, 1H), 4.98–4.93 (m, 1H), 4.00–3.94 (m, 1H), 3.26–3.21 (m, 1H), 3.14–3.09 (m, 1H), 2.89–2.83 (m, 1H), 2.74–2.64 (m, 1H), 2.35 (d, *J* = 12.8 Hz, 1H), 2.11 (d, *J* = 12.4 Hz, 1H), 1.79–1.75 (m, 5H), 1.57–1.43 (m, 2H), 1.32 (t, *J* = 6.5 Hz, 6H, 2 × CH_3), 1.27 (s, 3H, CH_3), 1.21 (s, 3H, CH_3). ^{13}C NMR (100 MHz, $CDCl_3$) δ 179.47, 169.84, 162.90 (^1J(C,F) = 243.2 Hz), 148.13, 145.69, 143.99, 140.05, 139.29 (^3J(C,F) = 10.8 Hz), 136.32, 129.85 (^3J(C,F) = 9.2 Hz), 129.57, 129.24, 128.90, 127.35, 124.76, 115.13 (^4J(C,F) = 2.5 Hz), 111.03 (^2J(C,F) = 21.3 Hz), 107.36 (^2J(C,F) = 26.0 Hz), 55.63, 47.39, 44.87, 38.01, 37.63, 37.38, 36.92, 29.73, 28.67, 25.01, 23.89, 23.85, 20.51, 18.38, 16.40. HR-MS (*m*/*z*) (ESI): calcd for $C_{35}H_{40}FN_2O_5S$ $[M - H]^-$: 619.2647; found: 619.2657.

Compound **9b**: Yields 68.9%, as a white solid. Mp: 121.8−126.4 °C. $[\alpha]_D^{20}$ = +12 (*c* 0.1, AcOEt) ^{1}H NMR (400 MHz, $CDCl_3$) δ 8.32 (d, *J* = 8.0 Hz, 1H), 8.15 (s, 1H), 7.87 (s, 1H), 7.36–7.23 (m, 5H), 7.18 (s, 1H), 7.06 (t, *J* = 7.8 Hz, 1H), 6.96 (t, *J* = 7.8 Hz, 1H), 6.85 (d, *J* = 8.0 Hz, 1H), 6.51 (d, *J* = 7.5 Hz, 1H), 4.93–4.88 (m, 1H), 4.05–3.91 (m, 1H), 3.77 (s, 3H, -OCH_3), 3.27–3.15 (m, 2H), 2.87–2.72 (m, 2H), 2.34 (d, *J* = 12.8 Hz, 1H), 2.09 (d, *J* = 12.6 Hz, 1H), 1.91–1.70 (m, 4H),

1.63–1.49 (m, 3H), 1.32 (t, *J* = 7.2 Hz, 6H, 2 × CH_3), 1.25 (s, 3H, CH_3), 1.21 (s, 3H, CH_3). ^{13}C NMR (100 MHz, $CDCl_3$) δ 178.23, 169.17, 148.34, 148.21, 145.57, 144.31, 139.92, 136.84, 129.53, 129.43, 128.86, 127.14, 124.78, 124.29, 121.06, 119.93, 110.17, 55.72, 55.55, 47.23, 44.53, 38.37, 37.69, 37.39, 36.99, 29.92, 28.64, 24.96, 23.91, 23.83, 20.14, 18.45, 16.46. HR-MS (*m*/*z*) (ESI): calcd for $C_{36}H_{43}N_2O_6S$ $[M - H]^-$: 631.2847; found: 631.2855.

Compound **9c**: Yields 63.7%, as a white solid. Mp: 160.6−166.8 °C. $[\alpha]_D^{20}$ = +40 (*c* 0.1, AcOEt) ^{1}H NMR (400 MHz, CDCl3) δ 8.87 (s, 1H,), 7.87 (s, 1H), 7.37 (d, *J* = 8.0 Hz, 2H), 7.29–7.24 (m, 3H), 7.21 (d, *J* = 7.6 Hz, 2H), 7.17–7.09 (m, 3H), 7.02 (t, *J* = 8.0 Hz, 1H), 6.70 (d, *J* = 8.0 Hz, 1H), 5.03–4.98 (m, 1H), 4.01–3.95 (m, 1H), 3.25–3.13 (m, 2H), 2.85–2.79 (m, 1H), 2.72–2.61 (m, 1H), 2.34 (d, *J* = 12.8 Hz, 1H), 2.12 (d, *J* = 10.7 Hz, 1H), 1.91–1.67 (m, 5H), 1.47–1.43 (m, 2H), 1.32 (d, *J* = 6.7 Hz, 6H, 2 × CH_3), 1.27 (s, 3H, CH_3), 1.21 (s, 3H, CH_3). ^{13}C NMR (100 MHz, $CDCl_3$) δ 179.03, 169.67, 148.21, 145.61, 144.07, 140.02, 137.63, 136.48, 129.55, 129.41, 128.89, 128.81, 127.26, 124.76, 124.50, 120.09, 55.35, 47.37, 44.79, 38.35, 37.64, 37.38, 36.91, 29.75, 28.66, 25.00, 23.89, 23.88, 20.50, 18.39, 16.41. HR-MS (*m*/*z*) (ESI): calcd for $C_{35}H_{41}N_2O_5S$ $[M - H]^-$: 601.2741; found: 601.2752.

Compound **9d**: Yields 67.9%, as a white solid. Mp: 121.3−125.6 °C. $[\alpha]_D^{20}$ = +38 (*c* 0.1, AcOEt) ^{1}H NMR (400 MHz, $CDCl_3$) δ 8.33 (d, *J* = 7.9 Hz, 1H), 8.07 (s, 1H), 7.88 (s, 1H), 7.29–7.25 (m, 5H), 7.17 (s, 1H), 7.08 (t, *J* = 7.7 Hz, 1H), 6.97 (t, *J* = 7.7 Hz, 1H), 6.86 (d, *J* = 8.0 Hz, 1H), 6.56 (d, *J* = 7.2 Hz, 1H), 4.90–4.85 (m, 1H), 4.01–3.95 (m, 1H), 3.77 (s, 3H), 3.18 (d, *J* = 7.0 Hz, 2H), 2.94–2.72 (m, 2H), 2.35 (d, *J* = 12.4 Hz, 1H), 2.10 (d, *J* = 12.4 Hz, 1H), 1.88–1.68 (m, 5H), 1.50–1.45 (m, 2H), 1.34–1.31 (m, 6H, 2 × CH_3), 1.29 (s, 3H, CH_3), 1.23 (s, 3H, CH_3). ^{13}C NMR (100 MHz, $CDCl_3$) δ 178.15, 169.16, 148.38, 148.14, 145.60, 144.29, 139.95, 136.56, 129.50, 129.40, 128.82, 127.16, 127.10, 124.78, 124.31, 121.11, 119.91, 110.14, 55.73, 55.44, 47.20, 44.67, 38.62, 37.70, 37.44, 37.13, 29.80, 28.65, 24.96, 23.92, 23.83, 20.54, 18.47, 16.53. HR-MS (*m*/*z*) (ESI): calcd for $C_{36}H_{43}N_2O_6S$ $[M - H]^-$: 631.2847; found: 631.2855.

Compound **9e**: Yields 66.1%, as a white solid. Mp: 178.5−183.6 °C. $[\alpha]_D^{20}$ = +9 (*c* 0.1, AcOEt) ^{1}H NMR (400 MHz, $CDCl_3$) δ 8.50 (s, 1H), 8.18 (t, *J* = 7.7 Hz, 1H), 7.86 (s, 1H), 7.33–7.21 (m, 5H),

7.15 (s, 1H), 7.12–6.99 (m, 3H), 6.43 (d, *J* = 7.1 Hz, 1H), 4.96 (d, *J* = 7.1 Hz, 1H), 4.01–3.95 (m, 1H), 3.30–3.25 (m, 1H), 3.19–3.14 (m, 1H), 2.88–2.70 (m, 2H), 2.32–2.28 (m, 1H), 2.10 (d, *J* = 12.1 Hz, 1H), 1.84–1.69 (m, 5H), 1.46–1.41 (m, 2H), 1.33 (d, *J* = 6.7 Hz, 6H, 2 × CH_3), 1.24 (s, 3H, CH_3), 1.20 (s, 3H, CH_3). ^{13}C NMR (100 MHz, $CDCl_3$) δ 178.99, 169.78, 152.85 (^1J(C,F) = 243.4 Hz), 148.26, 145.58, 144.25, 139.97, 136.38, 129.52, 129.30, 128.93, 127.33, 125.92 (^2J(C,F) = 10.6 Hz), 124.97 (^3J(C,F) = 7.5 Hz), 124.78, 124.56 (^3J(C,F) = 3.6 Hz), 122.27, 115.05 (^2J(C,F) = 19.0 Hz), 55.19, 47.31, 44.61, 37.64, 37.60, 37.38, 36.98, 29.73, 28.66, 25.02, 23.91, 23.87, 20.59, 18.41, 16.45. HR-MS (*m*/*z*) (ESI): calcd for $C_{35}H_{40}FN_2O_5S$ $[M - H]^-$: 619.2647; found: 619.2649.

Compound **9f**: Yields 51.4%, as a white solid. Mp: 180.3−187.8 °C. $[\alpha]_D^{20}$ = +7 (c 0.1, AcOEt) ^{1}H NMR (400 MHz, DMSO-d_6) δ 9.37 (s, 1H), 7.90–7.75 (m, 2H), 7.69–7.61 (m, 2H), 7.43–7.36 (m, 1H), 7.34–7.28 (m, 2H), 7.27–7.19 (m, 3H), 7.16–7.09 (m, 1H), 6.89 (s, 1H), 4.88–4.79 (m, 1H), 4.03–3.98 (m, 1H), 3.22–3.18 (m, 1H), 3.09–3.03 (m, 1H), 2.61–2.55 (m, 1H), 2.44–2.31 (m, 1H), 2.17 (d, *J* = 11.9 Hz, 1H), 1.90–1.86 (m, 1H), 1.68–1.51 (m, 4H), 1.46–1.24 (m, 3H), 1.14–1.08 (m, 12H, 4 × CH_3). ^{13}C NMR (100 MHz, DMSO-d_6) δ 178.53, 171.14, 146.04, 143.70, 142.57, 138.55, 136.40, 136.23, 133.14, 129.74, 129.53, 128.63, 128.47, 126.96, 126.76, 126.73, 125.48, 122.72, 116.48, 55.50, 46.97, 44.85, 38.02, 37.00, 36.99, 36.71, 28.99, 28.05, 25.14, 24.68, 24.40, 20.73, 18.71, 16.78. HR-MS (*m*/*z*) (ESI): calcd for $C_{35}H_{40}BrN_2O_5S$ $[M - H]^-$: 679.1846; found: 679.1857.

Compound **9g**: Yields 52.7%, as a white solid. Mp: 181.1−187.2 °C. $[\alpha]_D^{20}$ = +38 (*c* 0.1, AcOEt) ^{1}H NMR (400 MHz, DMSO-d_6) δ 14.50 (s, 1H), 9.41 (s, 1H), 7.93–7.75 (m, 1H), 7.68–7.62 (m, 1H), 7.63 (d, *J* = 3.4 Hz, 1H), 7.40 (d, *J* = 7.6 Hz, 1H), 7.37–7.34 (m, 1H), 7.32–7.18 (m, 3H), 7.16–7.10 (m, 1H), 6.87 (d, *J* = 4.1 Hz, 1H), 4.90–4.72 (m, 1H), 4.05–3.98 (m, 1H), 3.22–3.17 (m, 1H), 3.10–3.01 (m, 1H), 2.63–2.53 (m, 1H), 2.44–2.32 (m, 1H), 2.17 (d, *J* = 12.0 Hz, 1H), 2.02–1.86 (m, 1H), 1.59–1.50 (m, 2H), 1.41–1.28 (m, 3H), 1.13–1.08 (m, 12H). ^{13}C NMR (100 MHz, DMSO-d_6) δ 178.56, 171.17, 145.98, 143.69, 142.88, 138.57, 136.41, 136.04, 133.17, 129.76, 129.54, 128.66, 128.49, 126.98, 126.75, 125.52, 122.72, 116.50, 55.50, 46.98, 44.87,

38.04, 37.00, 36.71, 36.42, 28.98, 28.02, 25.15, 24.71, 24.42, 20.74, 18.72, 16.79. HR-MS (*m/z*) (ESI): calcd for $C_{35}H_{40}BrN_2O_5S$ $[M - H]^-$: 679.1846; found: 679.1858.

Compound **9h**: Yields 69.9%, as a white solid. Mp: 178.0−182.9 °C. $[\alpha]_D^{20}$ = +43 (*c* 0.1, AcOEt) ^{1}H NMR (400 MHz, $CDCl_3$) δ 8.29 (s, 1H), 8.19 (t, *J* = 7.9 Hz, 1H), 7.84 (s, 1H), 7.37–7.31 (m, 2H), 7.29 (d, *J* = 5.0 Hz, 3H), 7.15 (s, 1H), 7.13–7.09 (m, 1H), 7.06–7.02 (m, 2H), 6.33 (d, *J* = 7.2 Hz, 1H), 4.90–4.84 (m, 1H), 3.98–3.91 (m, 1H), 3.30–3.25 (m, 1H), 3.18–3.12 (m, 1H), 2.79–2.75 (m, 2H), 2.31 (d, *J* = 13.0 Hz, 1H), 2.05 (d, *J* = 10.6 Hz, 1H), 1.76–1.64 (m, 5H), 1.56–1.44 (m, 2H), 1.30 (t, *J* = 7.2 Hz, 6H, 2 × CH_3), 1.19 (s, 3H, CH_3), 1.17 (s, 3H, CH_3). ^{13}C NMR (100 MHz, $CDCl_3$) δ 178.94, 169.48, 152.65 (^1J(C,F) = 243.3 Hz), 148.14, 145.49, 144.08, 139.81, 136.52, 129.41, 129.22, 128.94, 127.26, 125.83 (^2J(C,F) = 10.3 Hz), 124.82 (^3J(C,F) = 7.4 Hz), 124.69, 124.47 (^3J(C,F) = 3.7 Hz), 121.92, 114.97 (^2J(C,F) = 19.0 Hz), 55.40, 47.19, 44.35, 37.49, 37.31, 37.25, 36.76, 29.77, 28.55, 24.85, 23.82, 23.75, 19.99, 18.27, 16.31. HR-MS (*m/z*) (ESI): calcd for $C_{35}H_{40}FN_2O_5S$ $[M - H]^-$: 619.2647; found: 619.2653.

Compound **9i**: Yields 65.9%, as a white solid. Mp: 124.5−128.3 °C. $[\alpha]_D^{20}$ = +46 (*c* 0.1, AcOEt) ^{1}H NMR (400 MHz, $CDCl_3$) δ 8.87 (s, 1H), 7.86 (s, 1H), 7.29–7.24 (m, 7H), 7.13 (s, 1H), 6.83 (d, *J* = 7.5 Hz, 1H), 6.75 (d, *J* = 9.0 Hz, 2H), 5.15–5.02 (m, 1H), 3.96 (m, 1H), 3.77 (s, 3H), 3.24 (m, 1H), 3.15 (m, 1H), 2.64–2.80 (m, 2H), 2.32 (d, *J* = 11.9 Hz, 1H), 2.10–2.00 (m, 1H), 1.68–1.39 (m, 7H), 1.31 (m, 6H, 2 × CH_3), 1.23 (s, 3H, CH_3), 1.17 (s, 3H, CH_3). ^{13}C NMR (100 MHz, $CDCl_3$) δ 178.91, 169.73, 156.51, 148.19, 145.46, 144.08, 139.82, 136.93, 130.63, 129.46, 129.36, 128.62, 126.99, 124.65, 121.88, 114.01, 55.45, 55.42, 47.10, 44.47, 38.30, 37.57, 37.28, 36.75, 29.82, 28.55, 24.92, 23.82, 23.76, 20.05, 18.28, 16.37. HR-MS (*m/z*) (ESI): calcd for $C_{36}H_{43}N_2O_6S$ $[M - H]^-$: 631.2847; found: 631.2850.

4.4 Inhibition of Matrix Metalloproteinase Activity assay

MMPs inhibition assays were carried out in 50 mM Tris/HCl buffer, pH 6.8, 10 mM $CaCl_2$ at 25 °C as described previously [37]. Assays were performed with a fluorogenic substrate McaPro-Leu-Gly-Leu-Dpa-Ala-Arg-NH2 (13 μM) and human MMPs (nanomolar range concentration) from R&D Systems, except for human MMP-3, MMP-8, and MMP-9 described

above. Substrate and enzyme concentrations were kept well below 10% substrate utilization to ensure evaluation of initial rates. Briefly, MMP-3, -8, or -9 and test complexes at varying concentrations were pre-incubated at 37 °C for 30 min. Continuous assays were performed by recording the increase in fluorescence induced by the cleavage of fluorogenic substrates. Black, flat-bottomed, 96-well nonbinding surface plates (Corning-Costar, Schiphol-RijK, Netherlands) were used for this test. Fluorescence changes were monitored using a Fluoroskan Ascent microplate reader (Infinite M1000 Pro, Tecan US, Morrisville, NC) equipped with excitation and emission wavelengths of 325 and 393 nm, respectively. IC_{50} values of inhibitors were obtained with iterative fitting package (GraphPad Prism software).

4.5 Molecular docking

All the docking studies were carried out using Sybyl-X 2.0 on a windows workstation. The crystal structure of the MMPs proteins were retrieved from the RCSB Protein Data Bank (MMP-3: 1SLN) [38]. The synthetic analogues **8** and **9** were selected for the docking studies. The 3D structures of these selected compounds were first built using Sybyl-X 2.0 sketch followed by energy minimization using the MMFF94 force field and Gasteiger-Marsili charges. We employed Powell's method for optimizing the geometry with a distance dependent dielectric constant and a termination energy gradient of 0.005 kcal/mol. All the selected compounds were automatically docked into the binding pocket of MMPs by an empirical scoring function and a patented search engine in the Surflex docking program. Before the docking process, the natural ligand was extracted; the water molecules were removed from the crystal structure. Subsequently, the protein was prepared by using the Biopolymer module implemented in Sybyl. The polar hydrogen atoms were added. The automated docking manner was applied in the present work. Other parameters were established by default to estimate the binding affinity characterized by the Surflex-Dock scores in the software. Surflex-Dock total scores, which were expressed in -log10 (Kd) units to represent binding affinities, were applied to estimate the ligand-receptor interactions of newly designed molecules. A higher score represents stronger binding affinity. The optimal binding pose of the docked compounds was selected based on the Surflex scores and visual inspection of the docked complexes.

4.6 Cytotoxicity assay

The cell lines NCI-H460, HepG2, SKOV-3, MCF-7 and HL-7702 were obtained from the Shanghai Cell Bank in the Chinese Academy of Sciences. NCI-H460, HepG2, SKOV-3, MCF-7 and HL-7702 cell lines were grown on 96-well microtitre plates at a cell density of 10×10^5 cells/well in DMEM medium with 10% FBS. DMEM and FBS were obtained from Gibco-Thermo (BRL Co. Ltd., USA). The plates were incubated at 37°C in a humidified atmosphere of 5% CO_2/95% air for overnight. Therewith, the cells were exposed to different concentrations of target compounds, 5-FU and DOX, and incubated for another 48 h. The cells were stained with 10 μl of MTT at incubator for about 4 h. The medium was thrown away and replaced by 100 mL DMSO. The O. D. Value was read at 570/630 nm enzyme labeling instrument.

4.7 In vitro cell migration assay/wound healing assay

HepG2 cells (5×10^5 cells/well) were cultured in 6 well plates as confluent monolayers for 24 h. Then artificial scratch on the monolayers were created with 200 mL sterile pipette tip and washed twice with PBS to remove non-adherent cells. The media containing 5 μM and 10 μM of compound **8k** or without compound **8k** were added to each well. The migration of cells across the scratched area were photographed by using phase contrast microscope (Nikon) at 0 h (immediately), 24 h and 48 h time interval after treatment in three or more randomly selected fields.

4.8 Cell cycle analysis

The HepG2 cells line were treated with different concentrations of compound **8k**. After 24 h of incubation, cells were washed twice with ice-cold PBS, fixed and permeabilized with ice-cold 70% ethanol at -20°C overnight. The cells were treated with 100 μg /ml RNase A at 37°C for 30 min after washed with ice-cold PBS, and finally stained with 1 mg/ml propidium iodide (PI) (BD, Pharmingen) in the dark at 4°C for 30 min. Analysis was performed with the system software (Cell Quest; BD Biosciences).

4.9 Apoptosis analysis

HepG2 cells were seeded at the density of 2×10^6 cells/mL of the DMEM medium with 10%

FBS on 6-well plates to the final volume of 2 mL. The plates were incubated for overnight and then treated with different concentrations compound **8k** for 24 h. Briefly, after treatment with compound **8k** for 24 h, cells were collected and washed with PBS twice, and then resuspend cells in 1×Binding Buffer (0.1 M Hepes/NaOH (pH 7.4), 1.4 M NaCl, 25 mM $CaCl_2$) at a concentration of 1× 10^6 cells /ml. The cells were subjected to 5 μL of FITC Annexin V and 5 μL propidium iodide (PI) staining using annexin-V FITC apoptosis kit (BD, Pharmingen) followed the 100 μL of the solution was transfer to a 5 mL culture tube and incubate for 30 min at RT (25°C) in the dark. The apoptosis ratio was quantified by system software (Cell Quest; BD Biosciences).

4.10 AO/EB Staining

The AO/EB molecular probes were also used to detect apoptotic cells. HepG2 cells (1×10^6 cells) were seeded in six-well tissue culture plates. Following incubation, the medium was removed and replaced with fresh medium plus 10% fetal bovine serum and treated with 5 μM and 10 μM of compound **8k** for 24 h. After the treatment period, briefly, the cells were harvested, suspended in PBS, stained with 2 μL of AO/EB stain (100 mg/mL) at room temperature for 20 minutes. Fluorescence was read on a Nikon ECLIPSETE2000-S fluorescence microscope (OLYMPUS Co., Japan).

4.11 Statistics

The data were processed by the Student' st -test with the significance level $P\leq0.05$ using SPSS.

Acknowledgements

This study was supported by the National Natural Science Foundation of China (No. 81260472 21362002 and 21431001), Special Research Found for the Doctoral Program of Higher Education (NO. 20134504110002), State Key Laboratory for Chemistry and Molecular Engineering of Medicinal Resources, Ministry of Science and Technology of China (CMEMR2016-B06).

References

1. J. Fidler, M. L. Kripke, Metastasis results from preexisting variant cells within a malignant

tumor, Science, 197 (1997) 893-895.

2. Peter Friedl, Katarina Wolf, Tumour-cell invasion and migration: diversity and escapa mechanisms, Nat. Rev. Cancer, 3 (2003) 362-374.
3. S. Zucker, J. Vacirca, Role of matrix metalloproteinases (MMPs) in colorectal cancer, Cancer Metast. Rev., 23 (2004) 101-117.
4. D. A. Fishman, Y. Liu, S. M. Ellerbroek, M. S. Stack, Lysophosphatidic acid promotes matrix metalloproteinase (MMP) activation and MMP-dependent invasion in ovarian cancer cells, Cancer Res., 61 (2001) 3194-3199.
5. M. Tester, N. Ruangpani, R. L. Anderso, E. W. Thompson, MMP-9 secretion and MMP-2 activation distinguish invasive and metastatic sublines of a mouse mammary carcinoma system showing epithelial–mesenchymal transition traits. Clin. Exp. Metastasis. 18 (2000) 553–560.
6. Stewart Wylie, Ian C. MacDonald, Hemanth J. Varghese, Eric E. Schmidt, Vincent L. Morris, Alan C. Groom, Ann F. Chambers, The matrix metalloproteinase inhibitor batimastat inhibits angiogenesis in liver metastases of B16F1 melanoma cells, Clin. Exp. Metastasis, 17 (1999) 111–117.
7. M. Egeblad, Z. Werb, New functions for the matrix metalloproteinases in cancer progression, Nat. Rev. Cancer, 2 (2002) 161−174.
8. C. Gialeli, A. D. Theocharis, N. K. Karamanos, Roles of matrix metalloproteinases in cancer progression and their pharmacological targeting, FEBS J. 278 (2011) 16−27.
9. N. Robichaud, S. V. del Rincon, B. Huor, T. Alain, L. A. Petruccelli, J. Hearnden, C. Goncalves, S. Grotegut, C. H. Spruck, L. Furic, O. Larsson, W. J. Muller, W. H. Miller, N. Sonenberg, Phosphorylation of eIF4E promotes EMT and metastasis via translational control of SNAIL and MMP-3, Oncogene, 34 (2015) 2032–2042.
10. Becker, J. W.; Marcy, A. I.; Rokosz, L. L.; Axel, M. G.; Burbaum, J. J.; Fitzgerald, P. M. D.; Cameron, P. M.; Esser, C. K.; Hagmann, W. K.; Hermes, J. D.; Springer, J. P. Stromelysin-1: Three-dimensional structure of the inhibited catalytic domain and of the C-truncated proenzyme. Prot. Sci. 1995, 4, 1966-1976.
11. Faiz-Ur Rahman, Amjad Ali, Inam Ullah Khan, Hong-Quan Duong, Rong Guo, Hui Wang, Zhan-Ting Li, Dan-Wei Zhang, Novel phenylenediamine bridged mixed ligands dimetallic

square planner Pt(II) complex inhibits MMPs expression via p53 and caspasedependent signaling and suppress cancer metastasis and invasion, Eur. J. Med. Chem. 125 (2017) 1064-1075.

12. S. Zucker, J. Cao, W. T. Chen, Critical appraisal of the use of matrix metalloproteinase inhibitors in cancer treatment, Oncogene, 19 (2000) 6642−6650.
13. C. M. Overall, O. Kleifeld, Tumour microenvironment-opinion: validating matrix metalloproteinases as drug targets and antitargets for cancer therapy, Nat. Rev. Cancer, 6 (2006) 227−239.
14. R. E. Vandenbroucke, C. Libert, Is there new hope for therapeutic matrix metalloproteinase inhibition? Nat. Rev. Drug Discov., 13 (2014) 904−927.
15. L. M. Coussens, B. Fingleton, L.M. Matrisian, Matrix metalloproteinase inhibitors and cancer: trials and tribulations, Science, 295 (2002) 2387-2392.
16. Wen Gu, Ting-Ting Miao, Da-Wei Hua, Xiao-Yan Jin, Xu-Bing Tao, Chao-Bo Huang, Shi-Fa Wang, Synthesis and in vitro cytotoxic evaluation of new 1H-benzo[d]imidazole derivatives of dehydroabietic acid, Bioor. Med. Chem. Lett., 27 (2017) 1296–1300.
17. M. A. González, Aromatic abietane diterpenoids: their biological activity and synthesis, Nat. Prod. Rep., 32 (2015) 684-704.
18. M. A. González, Synthetic derivatives of aromatic abietane diterpenoids and their biological activities, Eur. J. Med. Chem., 87 (2014) 834-842.
19. M. W. Pertino, V. Verdugo, C. Theoduloz, G. Schmeda-Hirschmann, Synthesis and Antiproliferative Activity of Some Novel Triazole Derivatives from Dehydroabietic Acid, Molecules, 19 (2014) 2523-2535.
20. Xiao-Chao Huang, Meng Wang, Ying-Ming Pan, Gui-Yang Yao, Heng-Shan Wang, Xiao-Yan Tian, Jiang-Ke Qin, Ye Zhang, Synthesis and antitumor activities of novel thiourea α-aminophosphonates from dehydroabietic acid, Eur. J. Med. Chem., 69 (2013) 508-520.
21. Xiao-Chao Huang, Le Jin, Meng Wang, Dong Liang, Zhen-Feng Chen, Ye Zhang, Ying-Ming Pan, Heng-Shan Wang, Design, synthesis and in vitro evaluation of novel dehydroabietic acid derivatives containing a dipeptide moiety as potential anticancer agents, Eur. J. Med. Chem., 89 (2015) 370-385.
22. Xiaochao Huang, Rizheng Huang, Zhixin Liao, Yingming Pan, Shaohua Gou, Hengshan

Wang, Synthesis and pharmacological evaluation of dehydroabietic acid thiourea derivatives containing bisphosphonate moiety as an inducer of apoptosis, Eur. J. Med. Chem., 108 (2016) 381-391.

23. M. M. Ghorab, M. A. Shaaban, H. M. Refaat, H. I. Heiba, S. S. Ibrahim, Anticancer and radiosensitizing evaluation of some new pyranothiazole-Schiff bases bearing the biologically active sulfonamide moiety, Eur. J. Med. Chem., 53 (2012) 403-407.
24. Mostafa M. Ghorab, Fatma A. Ragab, Helmy I. Heiba, Marwa G. El-Gazzar, Sally S. Zahran, Synthesis, anticancer and radiosensitizing evaluation of some novel sulfonamide derivatives, Eur. J. Med. Chem., 92 (2015) 682-692.
25. Katia D'Ambrosio, Fatma-Zhora Smaine, Fabrizio Carta, Giuseppina De Simone, Jean-Yves Winum, Claudiu T. Supuran, Development of Potent Carbonic Anhydrase Inhibitors Incorporating Both Sulfonamide and Sulfamide Groups, J. Med. Chem. 55 (2012) 6776−6783.
26. Sérgio M. Marques, Elisa Nuti, Armando Rossello, Claudiu T. Supuran, Tiziano Tuccinardi, Adriano Martinelli, M. Amélia Santos, Dual Inhibitors of Matrix Metalloproteinases and Carbonic Anhydrases: Iminodiacetyl-Based Hydroxamate-Benzenesulfonamide Conjugates, J. Med. Chem., 51 (2008) 7968–7979.
27. N.C. Levitt, F.A. Eskens, K.J. O'Byrne, D.J. Propper, L.J. Denis, S.J. Owen, L. Choi, J.A. Foekens, S. Wilner, J.M. Wood, M. Nakajima, D.C. Talbot, W.P. Steward, A.L. Harris, J. Verweij, Phase I and pharmacological study of the oral matrix metalloproteinase inhibitor, MMI270 (CGS27023A), in patients with advanced solid cancer, Clin. Cancer Res., 7 (2001) 1912-1922.
28. Donald Bissett, Ken J. O'Byrne, J. von Pawel, Ulrich Gatzemeier, Allan Price, Marianne Nicolson, Richard Mercier, Elva Mazabel, Carol Penning, Min H. Zhang, Mary A. Collier, Frances A. Shepherd, Phase III Study of Matrix Metalloproteinase Inhibitor Prinomastat in Non–Small-Cell Lung Cancer, J. Clin. Oncol., 23 (2005) 842-849.
29. Yongseok Kwon, Jayoung Song, Honggu Lee, Eun-Yeong Kim, Kiho Lee, Sang Kook Lee, Sanghee Kim, Design, Synthesis, and Biological Activity of Sulfonamide Analogues of Antofine and Cryptopleurine as Potent and Orally Active Antitumor Agents, J. Med. Chem., 58 (2015) 7749–7762.

30. Eva M. Huber, Gerjan de Bruin, Wolfgang Heinemeyer, Guillem Paniagua Soriano, Herman S. Overkleeft, Michael Groll, Systematic Analyses of Substrate Preferences of 20S Proteasomes Using Peptidic Epoxyketone Inhibitors, J. Am. Chem. Soc., 137 (2015) 7835−7842.

31. Carmen Di Giovanni, Roberta Ettari, Serena Sarno, Archimede Rotondo, Alessandra Bitto, Francesco Squadrito, Domenica Altavilla, Tanja Schirmeister, Ettore Novellino, Silvana Grasso, Maria Zappala, Antonio Lavecchia, Identification of noncovalent proteasome inhibitors with high selectivity for chymotrypsin-like activity by a multistep structurebased virtual screening, Eur. J. Med. Chem., 121 (2016) 578-591.

32. Hacer Karatas, Elizabeth C. Townsend, Fang Cao, Yong Chen, Denzil Bernard, Liu Liu, Ming Lei, Yali Dou, Shaomeng Wang, High-Affinity, Small-Molecule Peptidomimetic Inhibitors of MLL1/WDR5 Protein−Protein Interaction, J. Am. Chem. Soc., 135 (2013) 669−682.

33. M. Al. H. Hassan, A.E. Fahamb, G. Mohamed, A.F. Khalid, Microwave irradiation: A facile, scalable and convenient method for synthesis of N-phthaloylamino acids, Arab. J. Chem. 5 (2012) 285-289.

34. L Chen, G Fang, X Wang, S Li, H Li, Surfactivity of the Bolaform Surfactant Disodium Sulfodehydroabietate, Chemistry and Industry of Forest Products, 1 (2008) 103-107.

35. Huang, W.; Meng, Q.; Suzuki, K.; Nagase, H.; Brew, K. Mutational Study of the Amino-Terminal Domain of Human Tissue Inhibitor of Metalloproteinases 1 (TIMP-1) Locates an Inhibitory Region for Matrix Metalloproteinases. J. Biol. Chem. 272 (1997) 22086−22091.

36. T.S. Reddy, H. Kulhari, V.G. Reddy, V. Bansal, A. Kamal, R. Shukla, Design, synthesis and biological evaluation of 1,3-diphenyl-1H-pyrazole derivatives containing benzimidazole skeleton as potential anticancer and apoptosis inducing agents, Eur. J. Med. Chem. 101 (2015) 790-805.

37. Dabert-Gay, A. S.; Czarny, B.; Devel, L.; Beau, F.; Lajeunesse, E.; Bregant, S.; Thai, R.; Yiotakis, A.; Dive, V. Molecular Determinants of Matrix Metalloproteinase-12 Covalent Modification by a Photoaffinity Probe: Insights into Activity-Based Probe Development and Conformational Variability of Matrix Metalloproteinases, J. Biol. Chem., 283 (2008)

31058−31067.

38. Becker, J.W., Marcy, A.I., Rokosz, L.L., Axel, M.G., Burbaum, J.J., Fitzgerald, P.M., Cameron, P.M., Esser, C.K., Hagmann, W.K., Hermes, J.D., Springer, J.P., Stromelysin-1: three-dimensional structure of the inhibited catalytic domain and of the C-truncated proenzyme, Protein Sci., 4 (1995) 1966-1976.

Schemes

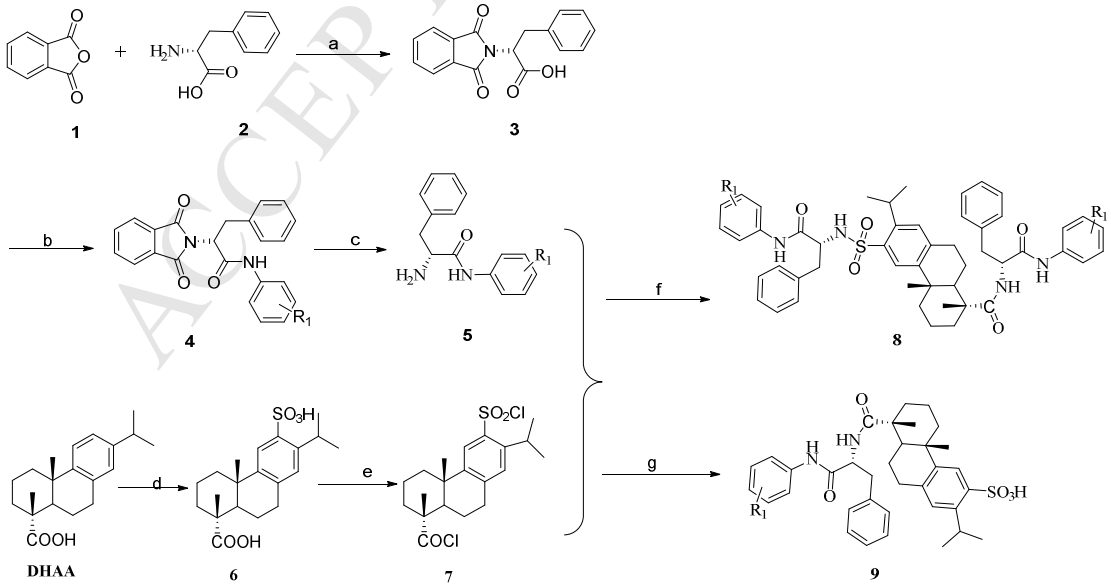

Scheme 1. Synthetic pathway to target compounds **8a**-**8u** and **9a**-**9i**. Reagents and conditions: (a) phthalic anhydride, CH_3COOH, 50□; (b) oxalyl chloride, CH_2Cl_2, aromatic primary amines, Et_3N,

r.t.; (c) hydrazine hydrate, CH_3OH; (d) H_2SO_4, r.t.; (e) oxalyl chloride, DMF, r.t.; (f) triethylamine, **7** and **5** (1:2), 18 h, r.t.; (g) triethylamine, **7** and **5** (1:1), 6 h, r.t.

Table 1. Inhibitory activities against MMP-3, -8 and -9 of target compounds

Compd.			IC_{50} (μM)[a]		
	L- and D-	R_1	MMP-3	MMP-8	MMP-9
8a	D-	4-F	59.7±0.5	92.1±0.6	>100
8b	D-	4-F-3-Cl	>100	>100	>100
8c	D-	3-F	>100	>100	>100
8d	D-	3-Br	>100	>100	>100
8e	L-	3-Br	39.7±0.6	87.5±0.3	93.1±0.9
8f	D-	H	19.6±0.5	52.5±0.2	53.6±0.7
8g	L-	H	8.8±0.3	28.2±0.2	24.3±0.9
8h	D-	3-OCH_3	40.8±0.6	76.5±0.1	83.4±0.2
8i	L-	3-OCH_3	22.6±0.2	55.1±0.9	51.9±0.6
8j	D-	3-CH_3	10.2±0.9	40.4±0.9	34.8±0.7
8k	L-	3-CH_3	0.4±0.1	6.6±0.1	8.8±0.6
8l	D-	4-OCH_3	24.9±0.5	56.1±0.6	57.8±0.5
8m	L-	4-OCH_3	21.3±0.7	52.1±1.0	54.6±0.6
8n	D-	4-CH_3	12.8±1.4	46.7±1.0	51.6±0.53
8o	L-	4-CH_3	1.0±0.3	17.7±0.5	20.9±1.2
8p	D-	2-F	35.3±0.4	64.5±0.8	66.6±0.9
8q	L-	2-F	25.5±0.1	41.5±0.6	48.3±0.3
8r	D-	2-OCH_3	30.2±0.4	52.5±0.4	56.2±0.4
8s	L-	2-OCH_3	23.8±0.2	43.0±0.9	43.9±0.1
8t	D-	2-CH_3	21.5±0.6	33.4±1.1	33. 6±0.7
8u	L-	2-CH_3	6.7±0.2	24.3±0.8	27.4±0.5
9a	L-	3-F	47.2±0.3	77.4±0.4	72.6±0.1
9b	D-	2-OCH_3	52.8±0.5	90.2±1.3	>100
9c	D-	H	26.9±0.8	89.3±0.6	95.9±0.3
9d	L-	2-OCH_3	>100	>100	>100
9e	D-	2-F	>100	>100	>100
9f	L-	2-Br	58.3±0.9	84.0±0.9	82.6±0.6
9g	D-	2-Br	>100	>100	>100
9h	L-	2-F	>100	>100	>100
9i	L-	4-OCH_3	28.0±0.3	39.4±0.4	36.3±0.2
CGS-27023A			0.03±0.04	0.01±0.02	0.01±0.03
DHAA	-	-	n.i.[b]	n.i.	n.i.

[a] IC_{50} against MMP-3, MMP-8 and MMP-9. [b] n.i. = no inhibition. Each value is the mean ± SD from triplicate assay in a single experiment.

Table 2. Docking scores (kcal/mol) for all studied compounds

Comd.	Total score	Crash	Polar	D_score	PMF_score	G_score	Chem score	Cscore
8a	6.02	-3.57	1.85	-178.96	-81.77	-386.39	-42.98	5
8b	3.49	-5.34	4.05	-166.26	-83.23	-342.73	-44.49	5
8c	4.90	-4.59	2.41	-180.80	-77.86	-357.83	-43.53	4
8d	3.41	-4.45	4.32	-185.36	-69.74	-331.28	-46.11	5
8e	5.97	-2.92	0.24	-137.88	-106.51	-313.38	-35.42	3
8f	6.69	-3.01	1.19	-179.10	-87.24	-374.56	-40.16	5
8g	7.83	-4.13	2.42	-184.08	-106.58	-380.48	-44.04	5
8h	5.68	-2.93	2.87	-188.87	-8.53	-393.74	-41.09	4
8i	6.64	-3.03	2.15	-152.25	-46.37	-324.78	-36.94	4
8j	7.21	-3.50	3.59	-180.04	-66.33	-375.93	-41.65	5
8k	11.09	-2.54	4.63	-213.41	-107.42	-382.35	-53.08	5
8l	6.89	-2.75	2.62	-174.41	-40.03	-368.96	-38.95	4
8m	6.93	-2.60	1.32	-179.72	-52.26	-359.93	-38.17	3
8n	7.82	-2.55	1.05	-176.68	-76.47	-358.94	-37.44	5
8o	10.33	-2.68	3.79	-185.09	-60.00	-357.67	-46.05	4
8p	5.86	-4.71	1.66	-216.08	-67.85	-387.08	-38.79	5
8q	6.38	-2.51	2.04	-173.91	-104.60	-321.34	-41.46	5
8r	6.16	-2.66	-1.44	-153.92	-38.62	-396.93	-38.87	4
8s	6.90	-4.26	2.11	-179.94	-70.19	-406.50	-41.46	5
8t	6.60	-3.70	3.55	-177.42	-65.44	-364.69	-45.83	5
8u	9.76	-4.45	5.53	-195.75	-71.06	-388.37	-51.08	5
9a	5.93	-3.24	3.04	-150.19	-39.03	-282.67	-34.03	4
9b	5.65	-2.09	2.47	-127.49	-29.11	-260.77	-30.73	4
9c	6.21	-2.11	0.94	-141.11	-57.55	-276.69	-30.07	4
9d	4.88	-2.64	2.17	-114.16	-41.52	-226.97	-28.31	5
9e	5.27	-2.23	1.38	-142.51	-44.73	-291.83	-30.99	3
9f	5.62	-3.19	2.32	-157.64	-54.17	-309.83	-36.24	5

9g	4.96	-1.65	1.14	-130.09	-59.65	-238.09	-29.16	5
9h	4.32	-3.60	3.93	-185.49	-68.48	-320.07	-44.44	3
9i	6.52	-3.07	4.92	-198.41	-88.30	-371.35	-50.99	4
1SLN-ligand	12.85	-2.08	7.41	-29.69	-62.58	-301.85	-33.28	3

Table 3. Biological activity of compounds **8a-8u** and **9a-9i** against different cancer cell lines

Compd.	IC_{50} (μM)[a]				
	NCI-H460	HepG2	SKOV-3	MCF-7	HL-7702
8a	>50	>50	>50	>50	>50
8b	>50	>50	>50	>50	>50
8c	>50	>50	>50	>50	>50
8d	>50	>50	>50	>50	>50
8e	39.9±0.9	26.6±0.7	35.9±0.4	38.6±0.8	>50
8f	20.6±0.5	17.3±0.8	19.6±0.2	18.2±0.2	>50
8g	17.5±0.3	11.9±1.1	15.8±0.5	16.8±0.3	>50
8h	22.4±0.9	18.4±1.3	20.5±1.0	21.2±0.5	>50
8i	20.5±1.2	14.8±1.2	18.3±0.3	18.1±0.4	>50
8j	16.5±0.8	10.8±1.1	13.4±0.2	14.2±0.2	>50
8k	10.6±0.8	4.2±1.1	7.6±0.3	8.5±1.1	>50
8l	28.9±0.6	20.4±0.9	23.6±0.5	26.5±0.7	>50
8m	24.1±0.9	16.1±0.5	19.4±0.4	21.8±0.7	>50
8n	30.1±0.4	24.2±0.3	18.4±1.3	14.3±0.4	>50
8o	13.1±1.1	7.1±0.9	9.8±0.4	10.0±0.6	>50
8p	45.0±0.7	35.5±0.2	38.4±0.6	41.4±0.3	>50
8q	43.9±0.9	31.5±0.7	36.8±0.8	37.7±0.5	>50
8r	36.6±0.8	29.8±0.4	35.5±0.6	35.7±1.1	>50
8s	36.0±0.8	27.5±1.5	31.3±0.6	32.0±1.4	>50
8t	30.7±0.9	17.6±0.6	24.9±0.9	27.0±0.9	>50
8u	12.9±0.6	9.2±1.2	10.3±0.5	9.9±0.8	>50
9a	>50	40.4±0.8	45.7±0.8	48.3±0.3	>50
9b	47.4±1.0	43.4±0.9	47.4±0.9	45.3±1.2	>50
9c	37.1±0.7	33.1±0.6	37.9±0.8	36.7±1.1	>50
9d	46.3±0.7	42.3±0.5	45.5±0.7	45.3±1.2	>50
9e	>50	>50	>50	>50	>50
9f	47.6±1.4	42.8±1.3	>50	>50	>50
9g	>50	46.9±0.8	>50	>50	>50
9h	>50	>50	>50	>50	>50
9i	34.6±1.2	25.2±1.6	28.9±0.7	32.4±1.3	>50
DHAA	>50	>50	>50	>50	>50
5-FU	36.0±0.9	28.8±0.8	32.5±1.1	38.5±0.7	46.0±1.4

DOX	2.5±0.7	1.5±0.5	1.7±0.8	0.7±0.7	10.4±0.9

[α] IC_{50} values are presented as the mean ± SD (standard error of the mean) from three separated experiments.

Figures captions

Fig. 1 Chemical structures of sulfonamide-based MMP and CA inhibitors.

Fig. 2 Binding modes of compound **8k** and ligand in the active site of 1SLN, respectively. Ligands and the important residues for binding interactions are represented by stick and line models. The hydrogen bonds are shown as yellow dotted lines (color figure online).

Fig. 3 In vitro cell migration assay. HepG2 cells were treated with compound **8k** (5 μM and 10 μM) and artificial scratches were done with sterile 200 mL pipette. The images were captured by using a Nikon Te2000 deconvolution microscope (magnification 200×) at 0 h, 24 h and 48 h.

Fig. 4 Compound **8k** induced cell cycle arrest at G1/S phase. HepG2 cells were treated with 5 or 10 μM compound **8k** for 24 h. Cells were fixed, stained with propidium iodide (PI), and were assessed by flow cytometry. Cells untreated were used for comparison.

Fig. 5 Annexin V-FITC and PI staining to evaluate apoptosis in HepG2 cells following compound **8k** treatment. HepG2 cells were treated with **8k** (5 and 10 μM, for 24 h), incubated with annexin V-FITC and PI and analyzed using flow cytometry.

Fig. 6. Compound **8k** induced apoptotic in HepG2 cells were determined by AO/EB staining and were photographed via fluorescence microscopy. HepG2 cells were treated with **8k** (5 and 10 μM, for 24 h), incubated with AO/EB. Images were acquired using a Nikon Te2000 deconvolution microscope (magnification 200×).

Figures

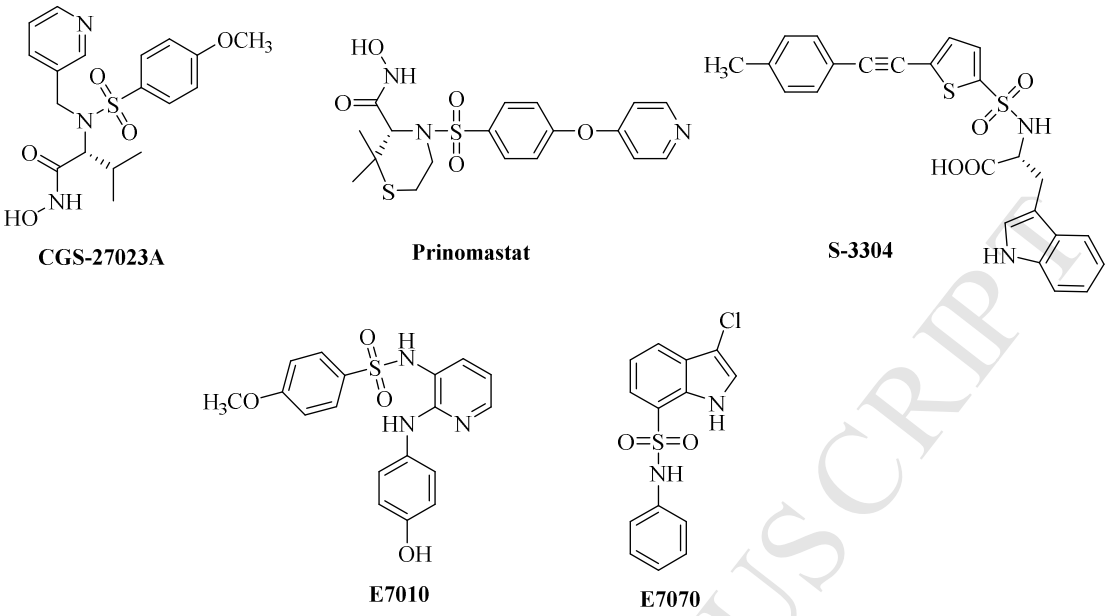

Fig. 1 Chemical structures of sulfonamide-based MMP and CA inhibitors.

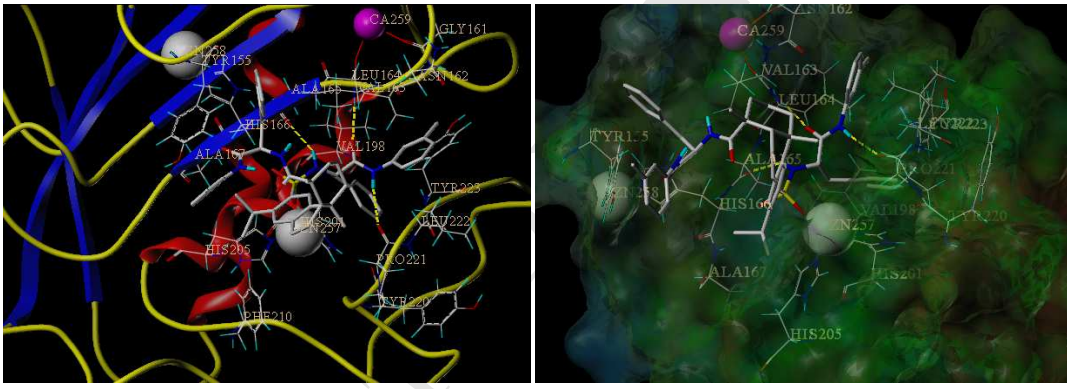

(a) **8k**

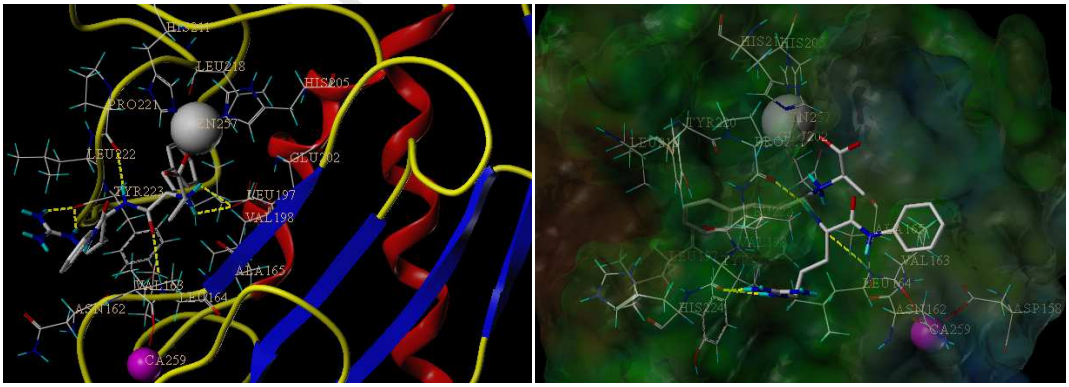

(b) **Ligand**

Fig. 2 Binding modes of compound **8k**, and ligand in the active site of 1SLN, respectively. Ligands and the important residues for binding interactions are represented by stick and line models. The hydrogen bonds are shown as yellow dotted lines (color figure online).

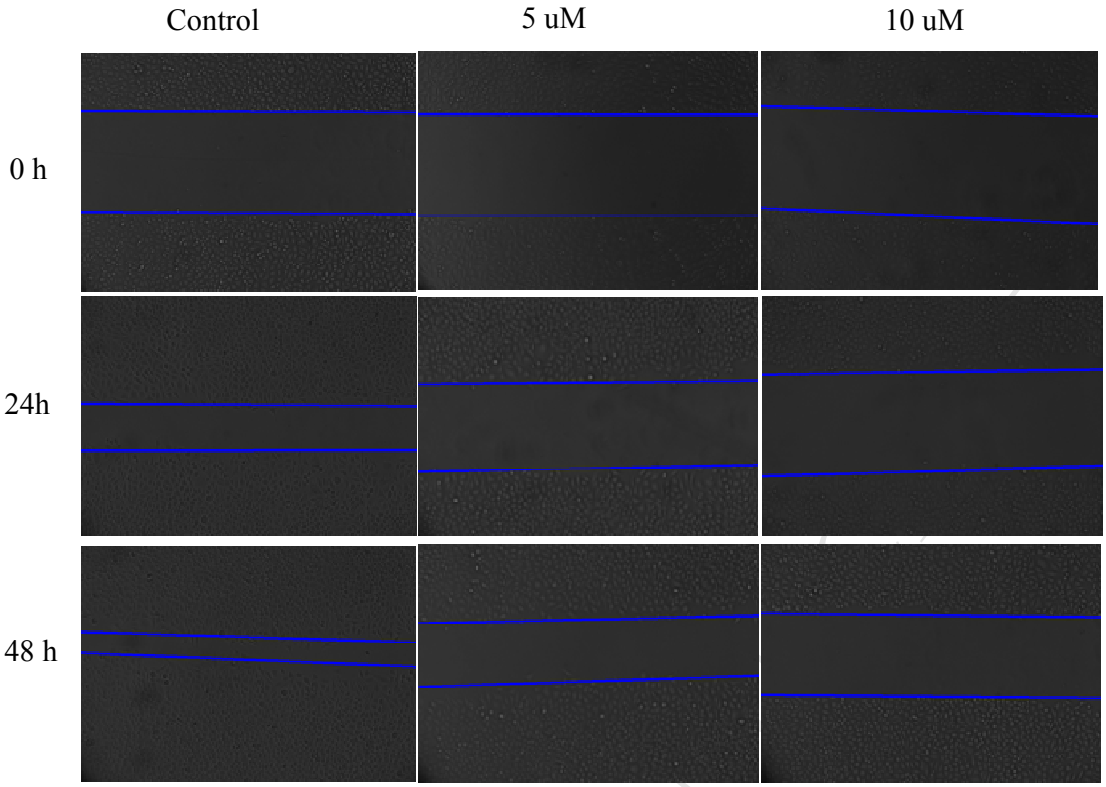

Fig. 3 In vitro cell migration assay. HepG2 cells were treated with compound **8k** (5 μM and 10 μM) and artificial scratches were done with sterile 200 mL pipette. The images were captured by using a Nikon Te2000 deconvolution microscope (magnification 200×) at 0 h, 24 h and 48 h.

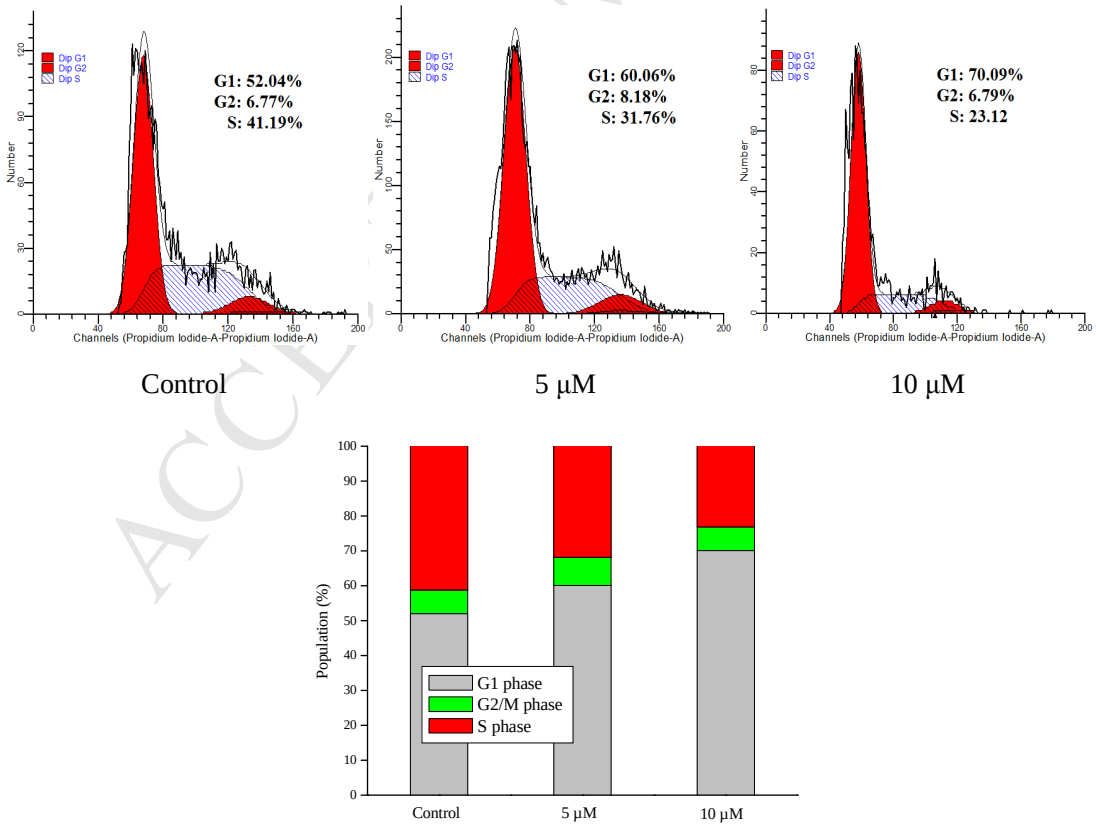

Fig. 4 Compound **8k** induced cell cycle arrest at G1/S phase. HepG2 cells were treated with 5 or

10 μM compound **8k** for 24 h. Cells were fixed, stained with propidium iodide (PI), and were assessed by flow cytometry. Cells untreated were used for comparison.

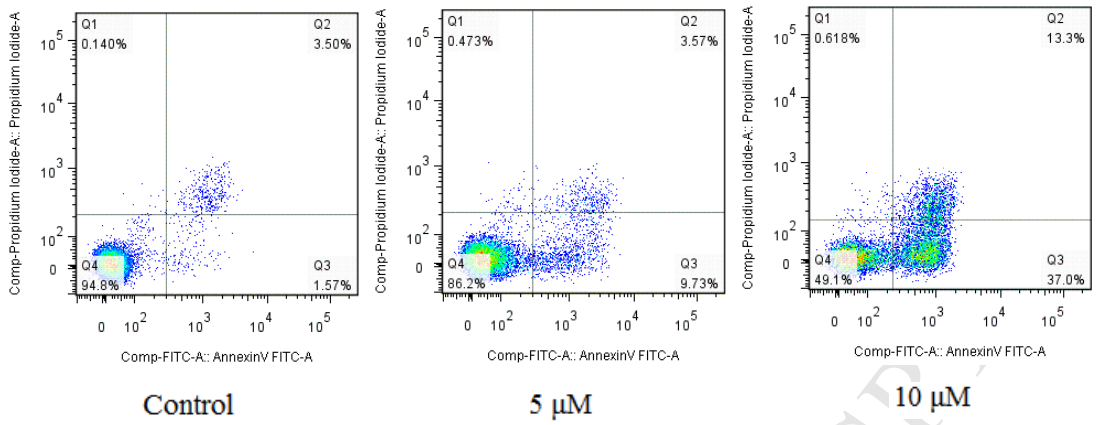

Fig. 5 Annexin V-FITC and PI staining to evaluate apoptosis in HepG2 cells following compound **8k** treatment. HepG2 cells were treated with **8k** (5 and 10 μM, for 24 h), incubated with annexin V-FITC and PI and analyzed using flow cytometry.

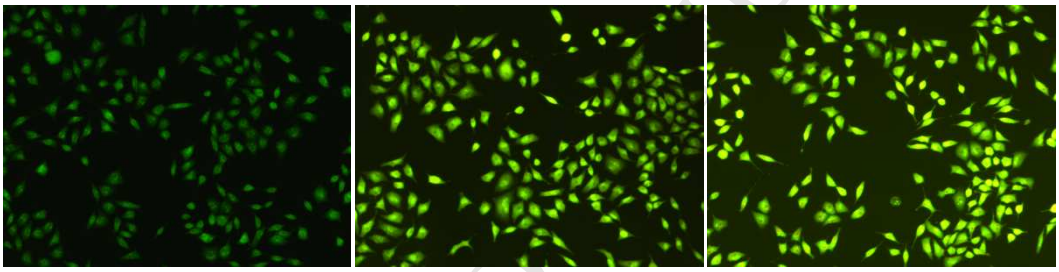

Fig. 6. Compound **8k** induced apoptotic in HepG2 cells were determined by AO/EB staining and were photographed via fluorescence microscopy. HepG2 cells were treated with **8k** (5 and 10 μM, for 24 h), incubated with AO/EB. Images were acquired using a Nikon Te2000 deconvolution microscope (magnification 200×).

Highlights

- A novel series of DHAA dipeptide derivatives containing the sulfonamide moiety were synthesized.
- Compound **8k** exhibited potential inhibitory activity against MMP-3.
- Molecular modeling suggested that **8k** tightly binds to the active site of MMP-3.
- The inhibitors efficiently inhibit the cell migration of human liver cancer cells.
- **8k** induced apoptosis and arrested cell cycle at G1 phase in HepG2 cells.